VON KARMAN INSTITUTE FOR FLUID DYNAMICS
CHAUSSEE DE WATERLOO, 72
B - 1640 RHODE SAINT GENESE, BELGIUM

PROJECT REPORT 1980-12 JUNE 1980

INVESTIGATION OF HEAT TRANSFER RATES ON A FILM COOLED FLAT PLATE WITH AND WITHOUT A PRESSURE GRADIENT

CENGIZ CAMCI

SUPERVISORS : P. LIGRANI
N. HAY

ACKNOWLEDGEMENTS

I wish to express my thanks to Dr. Ph. Ligrani VKI Assistant Professor and Dr. N. Hay,a visiting professor at VKI,for having given me the possibility to carry out this study and for their continious help and encouragement.

Thanks are also due to the laboratory staff of the VKI,especially to Mr. Rogier Conniasselle and Mr. Fernand Vande Broeck for their help and patience during the experimental work.

ABSTRACT

Heat transfer data for a film cooled flat plate with and without a pressure gradient is presented. The pressure gradient is the same as the one experienced at the endwall of a stationary turbine cascade. The VKI CT-2 compression tube facility is used for the tests and provides the same Reynolds numbers, Mach numbers and temperature ratios as found in a modern aircraft gas turbine. Heat transfer data was taken at three different blowing rates and three different coolant air temperature. Experimental results are presented in the form of adiabatic wall effectiveness distribution, isothermal wall effectiveness distribution, Stanton number distribution and heat transfer coefficient for film cooling. The present work also includes the calculated uncertainty values for the blowing parameter and Stanton numbers. Stanton numbers increased with the distance from the injection location and appeared to be recovering to no injection data far downstream of the last injection location. Adiabatic wall effectivenesses increased with increasing blowing rate. Decreasing coolant air temperatures increased isothermal effectiveness. Sellers' film superposition hypothesis gave about 10 percent underestimated adiabatic wall effectivenesses.

TABLE OF CONTENTS

LIST OF FIGURES

NON-ZERO PRESSURE GRADIENT TEST RESULTS

SINGLE ROW INJECTION TEST RESULTS

LIST OF SYMBOLS

q	Heat transfer rate with film cooling
q_o	Heat transfer rate without film cooling
h	Classical heat transfer coefficient
h_o	" " " " without injection
h_f	Heat transfer coefficient for film cooling
T_{rm}	Mainstream temperature
T_{aw}	Adiabatic wall temperature
T_w	Wall temperatue
T_{rc}	Coolant temperature
Θ	Non-dimensional coolant temperature
η	Adiabatic wall effectiveness
η_q	Isothermal wall effectiveness
M	Blowing parameter
C_d	Discharge coefficient
P_o	Test section total pressure (free stream)
T_o	Test section total temperature
P_∞	Free stream static pressure
P_{oc}	Plenum chamber pressure
P_{or1}	pressure /upstream of the inlet orifice
P_b	Pressure /upstream of the bleed orifice
$\dot{m}_{inj}$	Injection mass flow rate
$\dot{m}_b$	Bleed mass flow rate
ρ_∞	Free stream density
U_∞	Free stream velocity
A	Total injection area
$(\rho_\infty U_\infty)_c$	Coolant mass flow rate per unit area
γ	Specific heat ratio
R	Gas constant

r'	Resistance per unit length for the analogue
c'	Capacitance per unit length for the analogue
ρ	density
C_p	Specific heat
K	Thermal conductivity
α_R	Temperature constant
V_o	Set voltage for the heat transfer circuit
V_{out}	Analogue circuit output voltage
R_1	A resistance value for the analogue
R_o	Thin film resistance at ambient temperature
St	Stanton number
Ma	Mach number
Re	Reynolds number
Pr	Prandtl number
Nu	Nusselt number
x	coordinate or distance from the leading edge

1. INTRODUCTION

In recent years film cooling has been investigated for application to cool turbine blades and combustion chamber walls.Film cooling has been particularly succesful as a supplementary technique to internal convection cooling and impingement cooling to allow increased gas turbine inlet temperatures to be achieved.The film protects the surfaces from excessive heat by providing an insulating layer of cold fluid in the region very near the downstream of injection.The flow in this area is dominated by three dimensional turbulent mixing.

In this project,the effort has been devoted to obtain a set of heat transfer data on a film cooled flat plate, simulating the film cooled endwall of a stationary gas turbine cascade.The pressure over this film cooled flat plate was the same as the one experienced on the endwall of a turbine cascade which was investigated by Strunck (/).However ,flow over a flat plate shows a different structure as far as secondary flows are considered compared to the flow at the endwall of a stationary cascade.A typical film cooled endwall of a turbine cascade is given in fig.(1) .Each injection location consists of two rows of staggered injection holes with an inclination angle of 30 degrees.For this reason,the flat plate has 3 injection locations.

An analytical approach to heat transfer on a film cooled endwall is difficult from the viewpoint of present day numerical techniques and tools.A complete analytical solution of viscous 3D Navier-Stokes equations is required in this region,but not possible.Thus,in recent years,the shortest way to get a reliable set of heat transfer data has been an experimental approach.

1.1 PRIOR WORK

In 1976,Richards,Ville and Appels (2) investigated the film cooling effectiveness using the VKI CT-1 isentropic compression tube facility.They investigated the effect of curvature,Re number,Ma number and pressure gradient.Wall heat transfer and film cooling has been studied by Ville,Godard ,Richards and Sieverding (3).The authors experimentally confirmed that a linear relationship exists between classical convection heat transfer coefficient and nondimensional coolant temperature.Results were also presented for the variation of classical heat transfer coefficient with blowing parameter as well as lift off.Jabbari and Goldstein (4) studied the effect of injection angle and blowing rate.As the result of their study,theoretical models proposed to predict effectivenesses are in agreement with experimental data primarily at low values of blowing rate.They confirmed that the effect of interaction between the jets in the system with two staggered rows of holes is very important in increasing the efficiency particularly at higher blowing rates.The film cooling effectiveness of double rows of holes was investigated in a paper published by Afejuku,Hay and Lampard (5).They concluded that,the use of sellers' hypothesis to predict the effectiveness for high blowing rates gives values underpredicted,by about 10 percent. Adiabatic effectivenesses obtained by a mass transfer analogy decreased with increasing injection angle.Iso heat transfer lines are given at the endwall of a turbine cascade by Georgiou ,Godard and Richards (6).An experimental study of heat transfer and film cooling on large scale turbine endwalls has been carried out by Blair (7). Adiabatic wall effectivenesses have been measured by means of thermocouples which are located at the endwall.the author points out that the existance of the large vortex located in the corner between the endwall and the suction surfaces produces large variations of heat transfer in the trailing edge region.

Lander,Fish and Suo (8) performed experiments with film cooled first stage turbine vanes using two row discrete hole

cooling.Adiabatic wall effectivenesses were obtained using thermocouples.The authors observed the highest effectiveness levels at blowing rates of 0.5 ... 0.6 .The presence of film cooling holes on turbine airfoils increased the heat transfer even without blowing.The effect of large density differences between the mainflow and the secondary fluid on film cooling was studied by Pedersen, Eckert and Goldstein.They showed that the density ratio has a strong effect on the film cooling effectiveness for injection through holes, (9) .

In recent years,the cumulative effect of film cooling for multiple row injection systems were predicted using a superposition method called Sellers' hypothesis.Muska,Fish and Suo run experiments to prove the hypothesis,on flat plates and airfoils (10). With blowing rates from 0.1 to 1.3 and row spacings (16.7 ....25.0)xhole diameter .The additive film model provided good agreement between predicted and measured film effectivenesses for flat plate configurations.

In this project adiabatic wall effectivenesses and film cooling heat transfer coefficients were evaluated from wall heat flux,wall temperatures,free stream temperature and coolant temperature measurements.

1.2 TEST PROGRAM

In the experimental program,tests with a zero pressure gradient were carried out.For this configuration,Ma number was constant at a value of 0.42.Tests with a favorable pressure gradient were also carried out,using a curved top surface to create the pressure gradient.For these favorable pressure gradient tests, Ma numbers were varying from 0.22 to 0.77 in the flow direction.Single row injection was also used with a favorable pressure gradient.A schematic explaining the test program is given in fig.(2) .

During the tests free stream total temperature was about 395 ° K.Free stream total pressure was about 2.5 bar.For the present work the temperature and pressure conditions given above are

the representatives of 1365 °K and 8.75 bar actual engine conditions.A transient measurement technique were used.All the pressures,temperatures and heat fluxes were recorded by means of scopes,a U.V.chart recorder and an on line computer system.The data were sampled for 630 msec of a test.More about the simulation is given in append.(1) .Measurements and the data acqusition system is explained in chapter (3)

2. THEORY

Fig.(3) shows the basic heat transfer parameters of a film cooling system.There are two ways of defining a convective heat transfer coefficient for a film cooling system.The first definition is the classical approach,which may be given as

$$q = h.(T_{rm} - T_w) \qquad (1)$$

The second approach is related to adiabatic wall temperature.The adiabatic wall temperature is the temperature of the wall in the presence of a film with a zero heat flux condition.Using such an approach,the wall heat flux may be expressed using

$$q = h_f.(T_{aw} - T_w) \qquad (2)$$

where h_f is the convection heat transfer coefficient for film cooling.Non-dimensional coolant temperature for film cooling may be defined using

$$\theta = \frac{T_{rm} - T_{rc}}{T_{rm} - T_w} \qquad (3)$$

θ may then qualitatively be considered a measure of the coolant temperature with respect to the wall temperature. θ may vary from 1.1 to 1.8 in advanced high inlet temperature turbine designs.The adiabatic wall effectiveness may be given as,

$$\eta = \frac{T_{rm} - T_{aw}}{T_{rm} - T_{rc}} \qquad (4)$$

and is a function of film cooling hole configuration,coolant flow field and mainstream flow field. η =0 when adiabatic wall temperature is equal to mainstream gas temperature.

η has a max. value of unity for the case of equal coolant and adiabatic wall temperatures.A max. value of η means that the film is fully effective.Consequently,the adiabatic wall effectiveness has its higher values at just downstream of injection holes.As the boundary layer recovers to its undisturbed state ,for downstream of injection holes, η decreases in magnitude eventuall to zero.The film field containing the film cooling jets is three dimensional and complicated.Consequently,normal two dimensional boundary layer assumptions may no longer be considered applicable.

There is a linear relationship between h_f and h which was originally developed by Metzger (11).This relationship may be produced by first equating eq.(1) and eq.(2) to give

$$q = h(T_{rm} - T_w) = h_f(T_{aw} - T_w) \qquad (5)$$

Substituting the definitions of θ and ρ , T_{aw} may then be eliminated from eq.(5) such that,

$$q = h_f(T_{rm} - T_w)\cdot(1 - \rho\cdot\theta) \qquad (6)$$

without injection the heat flux is given by

$$q_o = h_o(T_{rm} - T_w) \qquad (7)$$

which,when combined with eq.(5) and eq.(6) results in

$$\frac{q}{q_o} = \frac{h}{h_o} = \frac{h_f}{h_o}(1 - \rho\cdot\theta) \qquad (8)$$

Eq.(8) then shows the linear dependence of h on θ .This linear relation is shown in fig.(4).Adiabatic wall effectiveness η and heat transfer coefficient for film cooling h_f can be determined from experimental data graphically by constructing the line,fig(4), from heat transfer data.Points A an B define $1/\eta$ and h_f/h at a given downstream location.The procedure

obtaining η and h_f/h_o is as follows.For a given coolant temperature, h/h_o may be determined by measuring wall heat flux,wall temperature and mainstream temperature,eq.(5) .This is repeated three times.By knowing points such as D,E and F a straight line may be constructed.Point A and B gives h_f/h and $1/\eta$ respectively.One also needs to measure h_o ,which is the classical heat transfer coefficient without injection.

The cooled surfaces of a high inlet temperature engine are not adiabatic surfaces.Isothermal conditions are more likely to exist due to large differences between the coolant,wall and mainstream temperature.Consequently,many designers use an isothermal wall effectiveness,defined using

$$\eta_q = 1 - \frac{q}{q_o} = 1 - \frac{h}{h_o} \qquad (9)$$

Substituting eq.(8) into eq.(9) then gives

$$\eta_q = 1 - \frac{h_f}{h_o}(1 - \eta\theta) \qquad (10)$$

which then shows that isothermal wall effectiveness is defined at a certain nondimensional coolant temperature level.In contrast adiabatic effectiveness is nondimensionalized with respect to temperature and thus does not require any further temperature specification.For a situation when the coolant temperature is less than the wall temperature,the direction of the heat flow will be from the wall to the film.For such a situation q may be less than zero and the isothermal effectiveness may have the values greater than unity.

3. EXPERIMENTAL FACILITIES AND TECHNIQUE

3.1 TEST FACILITY

The present test program was conducted in the VKI CT-2 compression tube facility.The CT-2 tunnel produces heat transfer power levels over short time intervals that are close to those in a real turbine. The light piston (27 kg.) isentropically compresses the air upstream of the test section.The tunnel is 1 m . in diameter and 5 m. long.It is supplied by the VKI 250 bar air supply reservoirs.The compressed air is released from the tube into the 25x10 cm test section.There is a gate valve between the test section and the tube.The valve operates pneumatically and has a 20x10 cm cross sectional area.Fast openin of the valve is achieved by the use of an exploding detonator. A dump tank of approximately 5 m^3 volume is situated downstream of the test section.The initial tube pressure and the initial dump tank pressure can be adjusted before the test in order to control Mach number,total temperature and total pressure over the test section.Total temperature can be varied from 290 ° K to 600 ° K.For this project a total temperature of 395 ° K was used.Total pressure was approximately 2.5 bar during the tests.The total temperature and pressure given above are the represantatives of 1365 ° K and 8.75 bar actual engine conditions.This simulation is explained in appendix (1).Test section total pressure and the heat transfer data sampled during the tests were transmitted to a PDP computer,using a 16 channel data acqusition system .More about the data acqusition system is presented in chapter 3.5 .The data related with the injection system and the static pressures over over the flat plate were taken using four oscilloscopes and a U.V. chart recorder.The free stream total pressure,pressure at the inlet orifice to the plenum chamber,bleed orifice pressures and plenum chamber pressure were measured in this way.Flat plate surface static pressure distributions were also taken using the oscilloscopes.Temperature data for free stream, inlet orifice to the plenum chamber,bleed orifices and plenum chamber were recorded by means of the U.V. chart recorder.

3.2 TEST SECTION

The film cooled flat plate used in this project is shown in fig.(5).The curved top surface was used to generate a favorable pressure gradient over the flat plate.For non-zero pressure gradient tests,a flat top surface was used.Wall heat fluxes were measured at 47 different downstream locations by means of thin film platinum heat transfer gauges.Locations for heat transfer measurements are shown in fig (6) .The heat transfer gauges were imbedded in a pyrex substrate which is a non-metallic material.

In fig.(6) , injection locations are labelled A,B and C . Each location consists of two rows of injection holes.The adjacent rows of injection holes are staggered with a total of 87 holes;44 in the upstream row and 43 in the downstream row.Additional details of the injection system configuration are presented in section 6.3 .

A boundary layer slot is located just upstream of the test section.The boundary layer over the test surface then develops from the leading edge of the flat plate shown in fig(6).The instrumented surface of the flat plate also includes a number of static pressure holes.After measurement of the static pressure distribution,the velocity and Mach number distributions may be determined along the test section.For this purpose steady,one dimensional, adiabatic flow of an ideal gas was assumed and using,

$$\frac{P_o}{P_\infty} = \left[1 + \frac{1}{5} M_\infty^2 \right]^{7/2} \qquad (11)$$

Mach numbers were calculated from measured static pressures.

3.3 INJECTION SYSTEM

A leakage type injection system was used for the experiments. The flushing time of the plenum chamber were calculated and found to be less than 5 msec.The injection system configuration is given in fig(7).One inlet pipe and two outlet pipes with sonic orifices were used to control the coolant injection mass flow rate.A schematic showing injection holes is given in fig(8).Mass flow rate through a sonic orifice can be calculated using,

$$\dot{m} = 4.0424 \times 10^{-3} \times \frac{\pi \cdot d^2}{4} \cdot \frac{P}{\sqrt{T}} \quad \text{kg/sec} \qquad (12)$$

(d in mm, P in bar, T in K)

The difference between the inlet mass flow rate and the outlet mas flow rate gives the amount of fluid injected through injection hol

$$\dot{m}_{inject} = \dot{m}_{inlet} - \dot{m}_{bleed} \qquad (13)$$

By knowing the total injection mass flow rate through three injection locations,it is possible to get the injection mass flow rate per unit area for the whole injection system.However,the injection through an individual pair of rows may not be determined in such a manner.

Blowing parameter is defined as the ratio of injection mass flow rate per unit area to free stream mass flow rate per uni area.

$$M = \frac{(\rho_\infty U_\infty)_{coolant,\,actual}}{\rho_\infty U_\infty} \qquad (14)$$

where $\rho_\infty U_\infty$ is free stream mass flow rate per unit area.Using perfect gas relation and the definition of Mach number

$$\rho_\infty U_\infty = \frac{P_\infty \times 10^5}{R\,T_\infty} \cdot Ma \cdot \sqrt{\gamma R T_\infty} \quad \frac{kg}{m^2 \cdot sec} \qquad (15)$$

(P_∞ in bar, T_∞ in K)

Variation of free stream mass flow rate per unit area is given in Table -I ,for a favorable pressure gradient test.

	FIRST INJ. LOCAT.	SECOND INJ. LOCAT.	THIRD INJ. LOCAT.	
x	82.	106.	129.	mm.
$\rho_\infty U_\infty$	262.	381.	458.	kg/m².sec
P_∞	2.33	2.09	1.85	bar

Table-I

For the case of favorable pressure gradient over the flat plate mainstream fluid properties varies from one injection location to another. Due to different free stream static pressures there are three different blowing parameters for a given plenum chamber pressure. Free stream static pressures are 2.3 bar, 2.09 bar and 1.85 bar for the first, second and third injection locations, respectively. In fig.(9) variation of blowing parameter with plenum chamber pressure is given for each of the injection locations.

Isentropic coolant mass flow rate per unit area through an injection pipe may be calculated using,

$$(\rho_\infty U_\infty)_{coolant,s} = P_\infty \times \left(\frac{P_{oc}}{P_\infty}\right)^{0.286} \times \left[1 - \left(\frac{P_{oc}}{P_\infty}\right)^{-0.286}\right]^{0.5} \cdot T_{oc}^{-0.5} \times 1.562 \times 10^{-4} \quad \frac{kg}{m^2.sec} \qquad (16)$$

equation (16) is based on an isentropic process between the plenum chamber conditions and free stream conditions. The actual mass flow rate per unit area for injection is less than $(\rho_\infty U_\infty)_{coolant,s}$ due to non-isentropic losses between the plenum chamber and free stream. Actual mass flow rate per unit area may also be calculated from sonic orifice measurements. With this information one can calculate the discharge coefficient for a given injection location. The discharge coefficient may then be expressed as :

$$C_d = \frac{(\rho_\infty U_\infty)_{coolant,actual}}{(\rho_\infty U_\infty)_{coolant,s}} \qquad (17)$$

or alternatively;

$$C_d = \frac{\frac{\dot{m}_{inlet} - \dot{m}_{bleed}}{A}}{(\rho_\infty U_\infty)_{coolant,s}} \qquad (18)$$

by substituting eq.(13) and eq.(16) into eq.(18)

$$C_d = \frac{\frac{4.0424\times10^{-3}}{A}\times\frac{\pi}{4}\left[d^2_{inlet}\cdot\frac{P_{inlet}}{\sqrt{T_{inlet}}} - 2\cdot d^2_{bleed}\cdot\frac{P_{bleed}}{\sqrt{T_{bleed}}}\right]}{P_{\infty}\cdot\left(\frac{P_{oc}}{P_{\infty}}\right)^{0.286}\cdot\left[1-\left(\frac{P_{oc}}{P_{\infty}}\right)^{-0.286}\right]\cdot T_{oc}^{-0.5}\times 1.562\times10^{4}}$$

using eq.(14) ,the blowing parameter can be rearranged to become

$$M = \frac{C_d\times(\rho_{\infty}U_{\infty})_{coolant,s}}{\rho_{\infty}U_{\infty}} \qquad (2$$

3.4. MEASUREMENTS

Wall heat fluxes,pressures and temperatures were measured by a transient technique.A schematic of the measurement chain is given in fig.(11).The sequence of various events during a test is controlled using a timing unit.First ,injection is started , after about 100 msec. the compression tube piston increases the pressure in the tube.As soon as a certain pressure level inside the tube is reached,the main air supply opens by means of an explosive device.The opening time of the valve is controlled pneumatically and is about 20-30 msec.The timing unit can be adjusted to meet the timing requirements of a specific test.

Pressure measurements were made at many locations.These locations are the plenum chamber,free stream,upstream of the inlet orifice,upstream of two bleed orifices and static pressure holes on the flat plate.Static hole locations are shown in fig.(12 Compression tube total pressure was also measured.Validyne variabl reluctance transducers and semiconductor type pressure transducers were used for pressure measurements.Free stream total pressure were measured by a total pressure probe.The compression tube initial pressure was measured using a mercury manometer.Typical pressure traces are given in fig.(13).Static pressures along the test section and free stream total pressure are shown.Total pres-

sure fluctuations in the test section may be seen in fig.(13). Uncertainty value for pressure measurements was about $\mp$ 0.1 bar for all the measurement locations,except upstream of the inlet orifice.Pressure uncertainty was about $\mp$ 0.5 bar at upstream of the inlet orifice,due to high pressure level at this location and insensitive scope pictures.

Temperature measurements were made at five locations.These locations are the plenum chamber,free stream,upstream of the inlet orifice to the plenum chamber, upstream of two bleed orifices.The temperatures were measured using thermo-coax elements.Typical temperature traces are shown in fig.(14).At the beginning of the test,injection is initiated.A sudden temperature jump due to sudden pressure increase (region-A) at the inlet orifice to the plenum chamber and inside the plenum chamber is apparent from the trace. The plenum chamber pressure reaches its steady value 300 msec after injection valve opening. The main flow valve (shutter valve) opens 300 msec. after injection valve opening and the free stream temperature raises as indicated by region B . The effect of valve opening on plenum chamber and bleed upstream temperatures is very small (region-c).Temperatures were measured about 150 msec after shutter opening.Uncertainty value for temperature measurements was about $\mp$ 2 °C .Heat fluxes along the flat plate were measured by thin film platinum heat transfer gauges.The heat flux measurement technique used for our experiments were developed by Schultz and Jones ref.(12) .The technique is based on the assumptions that the flow of heat into film substrate is similiar to that into a semiinfinite material.An electronic circuit providing constant collector current is used to supply the thin film platinum gauge.TEmperature variations sensed by the thin film platinum gauge is converted into heat flux variations by an electrical analogue circuit using the principle given above.Analogue circuit and constant current supply is given in fig.(15).Wall heat flux can be determined using,

$$q(t) = \sqrt{\rho c k} \times \sqrt{\frac{\Gamma'}{c'}} \times \frac{1}{\alpha_R \cdot V_0} \times \frac{V_{out}}{R_1} \qquad (21)$$

where,

$$\alpha_R = \frac{1}{R_0} \cdot \frac{\Delta R}{\Delta T} \qquad (22)$$

12 3

12.29

α_R is called temperature constant and R_o is the electrical resistance of thin film platinum at ambient temperature.By knowing the output voltage from the analogue circuit (V_{out}),wall heat flux may be evaluated from eq.(21) as a function of thermal properties of the substrate,temperature coefficient of the platinum gauge and electrical properties of the analogue. (r', c' and R_i)

3.5 DATA ACQUSITION and REDUCTION

During the tests,a 16 channel data acqusition system were used.The system consists of 16 sample and hold units,a multiplexer and an A/D (analogue to digital) converter.Total sampling frequency for all channels can be set as high as 50 KHz.For the present tests,the sampling frequency for each channel was set to 2.0 KHz.With this frequency 630 msec. of data may be stored on the computer.14 out of 16 channels were used for heat transfer signals.One channel was for free stream total pressure and the last one was for shutter trace which allows a determination of the beginning of main flow.A typical heat transfer trace ,a total pressure(free stream) and a shutter trace are given in fig.(16).In fig.(17), heat transfer signal decreases by time.The main reason is the increasing temperature of the test section during the test.Data has been reduced using several computer programs and then stored on floppy disks.

4. EXPERIMENTAL RESULTS

In fig.(17) the Stanton number distribution over the flat plate is shown.The experimental data is presented both for a zero pressure gradient and a favorable pressure gradient.Stanton numbers for zero pressure gradient appear to be slightly higher than the favorable pressure gradient data far downstream of the leading edge.Stanton number versus Reynolds number is given in fig.(18).The experimental heat transfer data were compared with a well known heat transfer theory given by Kays, ref.(13) .Experimental uncertainty for Stanton number measurements based on a 95 per cent confidence interval was approximately 15 percent.

Fig.(19) shows the Mach number distribution along the flat plate for zero pressure gradient and nonzero pressure gradient cases.In this figure,a theoretical Mach number distribution is given for a turbine endwall.The theoretical Ma number distribution is based on a Mårtensen calculation and given by Strunck; ref.( ) .Reynolds number distribution over the film cooled flat plate for the case of zero pressure gradient and nonzero pressure gradient is given in fig.(20)

For the tests with injection from three different locations;increasing coolant air temperatures increased Stanton numbers at low,medium and high blowing rates as shown in fig.(23)-(24)-(25) .A low blowing rate corresponds to a blowing rate of 0.75 ,a medium blowing rate corresponds to a blowing rate of 1.00 and a high blowing rate corresponds to a blowing rate of 1.25 .Blowing rates were obtained based on equation (20) given in chapter 3.3 .For the accelerated boundary layer case(non zero pressure gradient),blowing rates were changing from one injection location to another because of changing free stream static pressure. In this study,all the blowing rate data is referred to the mid injection location.The highest blowing rate were observed at the first injection location from the leading edge for the case of non-zero pressure gradient (accelerated boundary layer case).For a given coolant air temperature,decreasing blowing rates increased Stanton numbers.These tendencies were observed for both zero pressure gradient and non-zero pressure gradient tests;fig.(29)-(30)-(31)-(32) .

St numbers for the tests with triple injection appeared to be recovering to the St numbers for no injection at locations far downstream of the third set of injection holes.

Data scattering ,non-repeatibility and unexpected data trends were observed upstream of the first set of holes,in the St number distributions.A surface roughness, resulting from silver connections between platinum gauge and wires may be a reason for this scattering.In this region ,boundary layer is very thin and sensitive to such surface discontinuities.Another reason may be a calibration change because of changing thermal properties of the substrate material.This aging problem may be avoided by making a new calibration for this set of gauges.$\sqrt{\rho c k}$ value is mainly a function of gauge making process and may change by time as it is mentioned above.

Adiabatic wall effectivenesses for a zero pressure gradient and a non-zero pressure gradient were evaluated from experimental data.In fig.(21) η distribution for a triple injection system is shown as a function of the distance from the leading edge.The Ma number distribution for the data in fig.(21) is constant at a value of 0.42 .Generally η decreased with the downstream distance from a row of injection holes.Increasing blowing rates result in increasing η . η distribution were also obtained for a film cooled flat plate with a non-zero pressure gradient.Ma numbers were changing from 0.22 to 0.77 in the accelerated free stream along the flat plate.For the case of non-zero pressure gradient, the adiabatic wall effectiveness shows the same trend with respect to distance downstream of a row of injection holes and with blowing rate.Adiabatic wall effectiveness data for zero pressure gradient shown in fig.(21) and the data for a non-zero pressure gradient shown in fig.(26) were compared. η is higher when favorable pressure gradient exists along the flat plate than when a zero pressure gradient is present.

In fig.(22) the distribution of heat transfer coefficient for film cooling is given along the flat plate for the case of zero pressure gradient.Increasing blowing rates result in increasing h_f/h at a given value of α .When evaluating h_f/h and η values,the procedures given in section 2. was followed.However a slightly nonlinear dependence of h on θ occured far downstream of each injection location.Consequently,at such locations

,uncertainties for η and h_f/h increased because of the nonlinearity problem.However just downstream of the injection location the dependence of h on θ was more closely linear.As an example to this problem,two graphs are shown in fig.(27) and fig.(28). Fig.(27) is presented for far downstream of an injection location.Fig.(28) is for just downstream of an injection location.

In fig.(33) isothermal wall effectiveness distribution over the flat plate with triple row injection is shown for an accelerated boundary layer.Decreasing coolant temperature from 290 °K to 260 ° K increased η_q about 35 percent just downstream of the first injection location.Isothermal effectiveness decreased with the downstream distance from the injection locations.For the case of cold fluid injection into the boundary layer η_q values were found to be greater than one.This is due to the direction of the heat flow for this case.With an injection fluid cooler than the wall,heat flow occurs from the plate to the main flow as it is explained in chapter 2 .

Single row injection tests with the same favorable pressure gradient were performed.Adiabatic wall effectiveness and heat transfer coefficients for film cooling were evaluated from the heat transfer data.The distributions are given in fig.(34)-(35) and (36).According to Sellers film superposition hypothesis,the second and subsequent film behaves as if the free stream temperature were the adiabatic wall temperature which would result from the upstream injection locations.For a triple injection system, η may be predicted with this hypothesis without running triple injection experiments.With this hypothesis,effectivenesses were directly obtained from single row injection test results. In fig.(38) a schematic picture for this hypothesis is shown. Measured adiabatic wall effectivenesses were compared with predicted effectivenesses.Sellers hypothesis gave about 10 percent underestimated effectivenesses compared to triple row injection measurements with a favorable pressure gradient,for a blowing parameter of 1.0 , fig.(39) .

CONCLUSIONS

Heat transfer data obtained without injection shows good agreement with well known heat transfer theory . Stanton number data were taken in a zero pressure gradient are slightly higher than data from the favorable pressure gradient flow far downstream of the leading edge.As the result of tests with injection,Stanton numbers increase with the downstream distance from the injection locations,and appear to be recovering to no injection data, far downstream of the last injection location.The adiabatic film cooling effectiveness increase with increasing blowing rate for both zero pressure gradient and non-zero pressure gradient tests.Decreasing coolant air temperatures increases isothermal wall effectiveness.Sellers' film superposition hypothesis gives adiabatic wall effectiveness values of which are 10 per cent below experimental results. The first set of heat transfer gauges may require a calibration repeat to verify measurements since some data scattering and unexpected trends exist in this region.

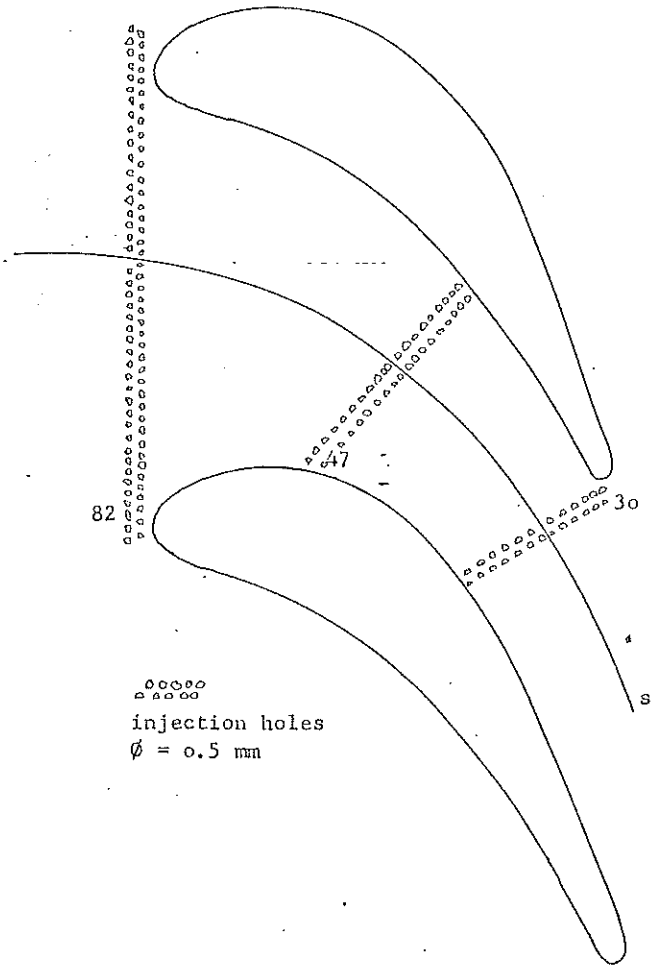

FIG.1

A TYPICAL FILM COOLED ENDWALL

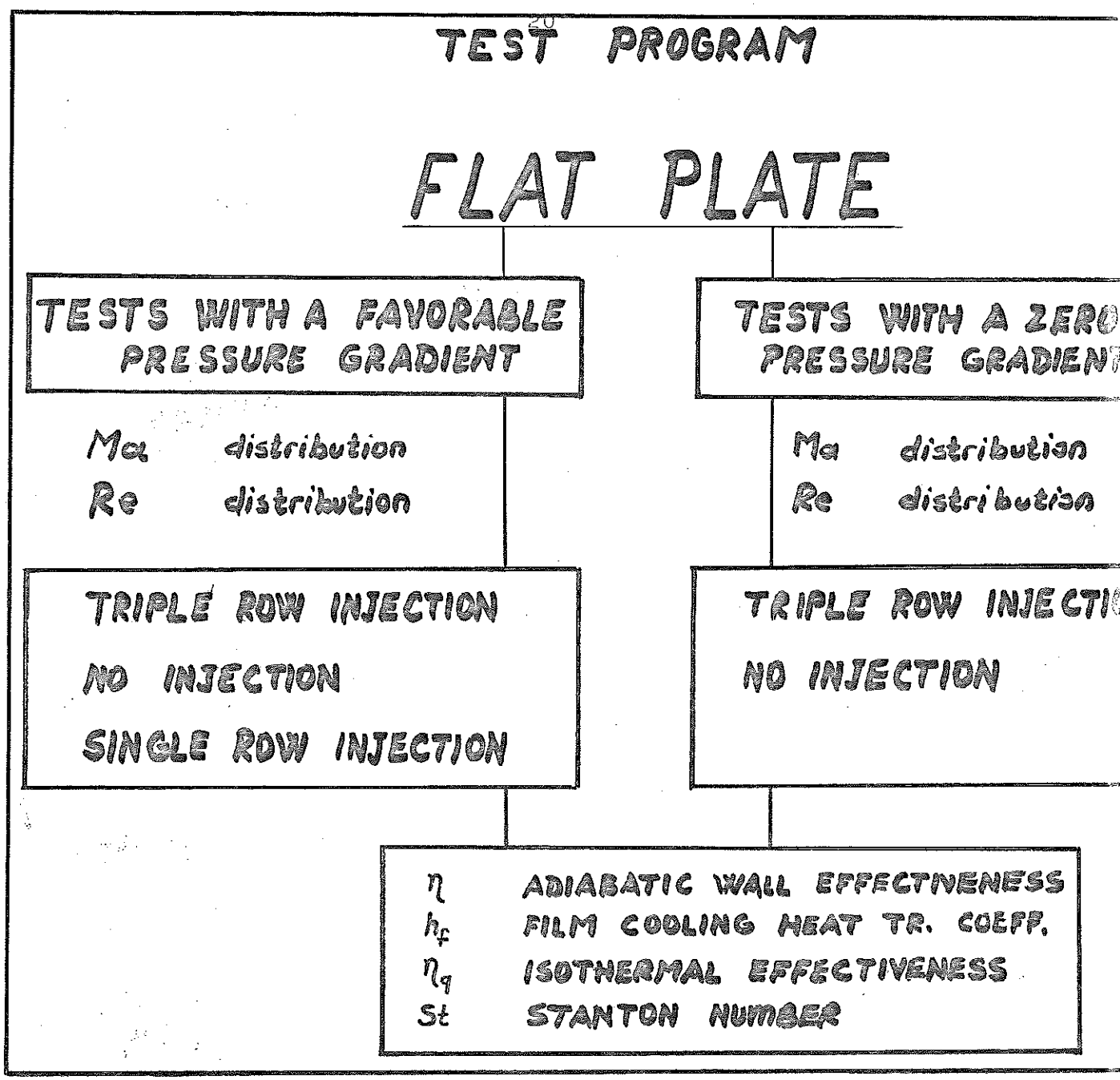

FIG.2

TEST PROGRAM

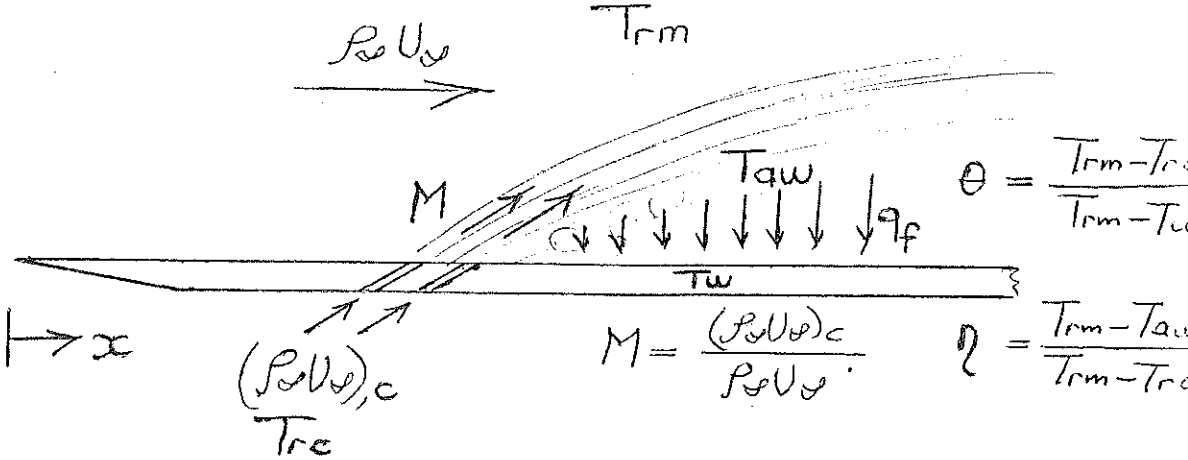

FIG.3

BASIC HEAT TRANSFER PARAMETERS OF A FILM COOLING SYSTEM

FIG.4

VARIATION OF HEAT TRANSFER COEFFICIENT

WITH NON-DIMENSIONAL COOLANT TEMPERATURE

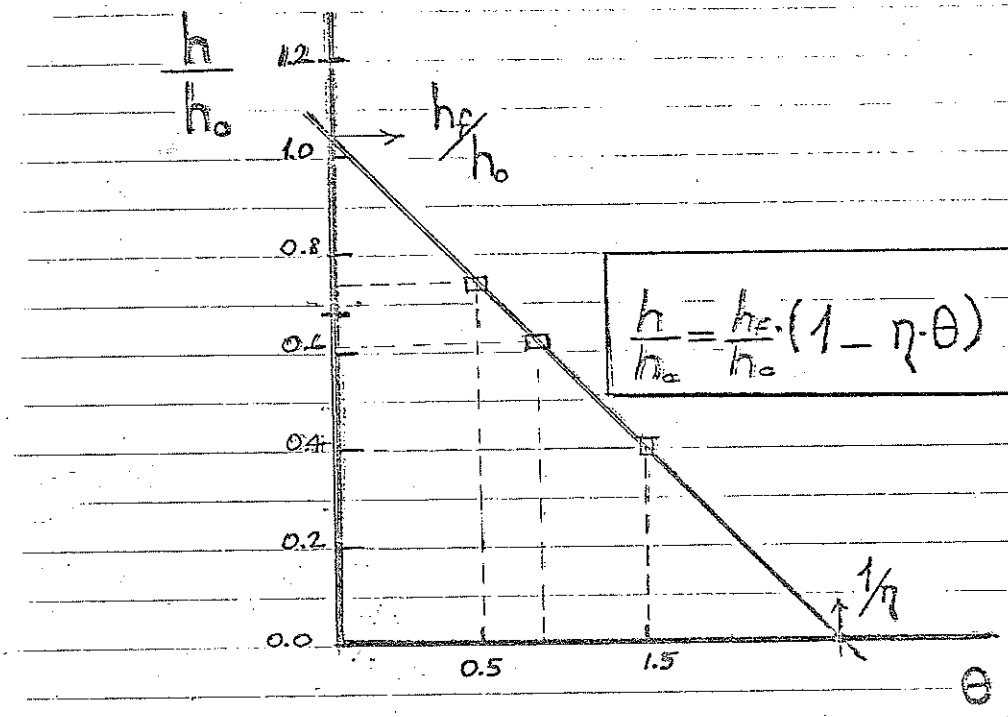

$$q_f = h_f (T_{aw} - T_w)$$

$$q_f = h (T_{rm} - T_w)$$

$$\Rightarrow h = h_f (1 - \eta\theta)$$

$$\eta = \frac{T_{rm} - T_{aw}}{T_{rm} - T_{rc}}$$

rm : recovery, mainstream
aw : adiabatic wall
rc : recovery coolant
w : wall

$$\theta = \frac{T_{rm} - T_{rc}}{T_{rm} - T_w}$$

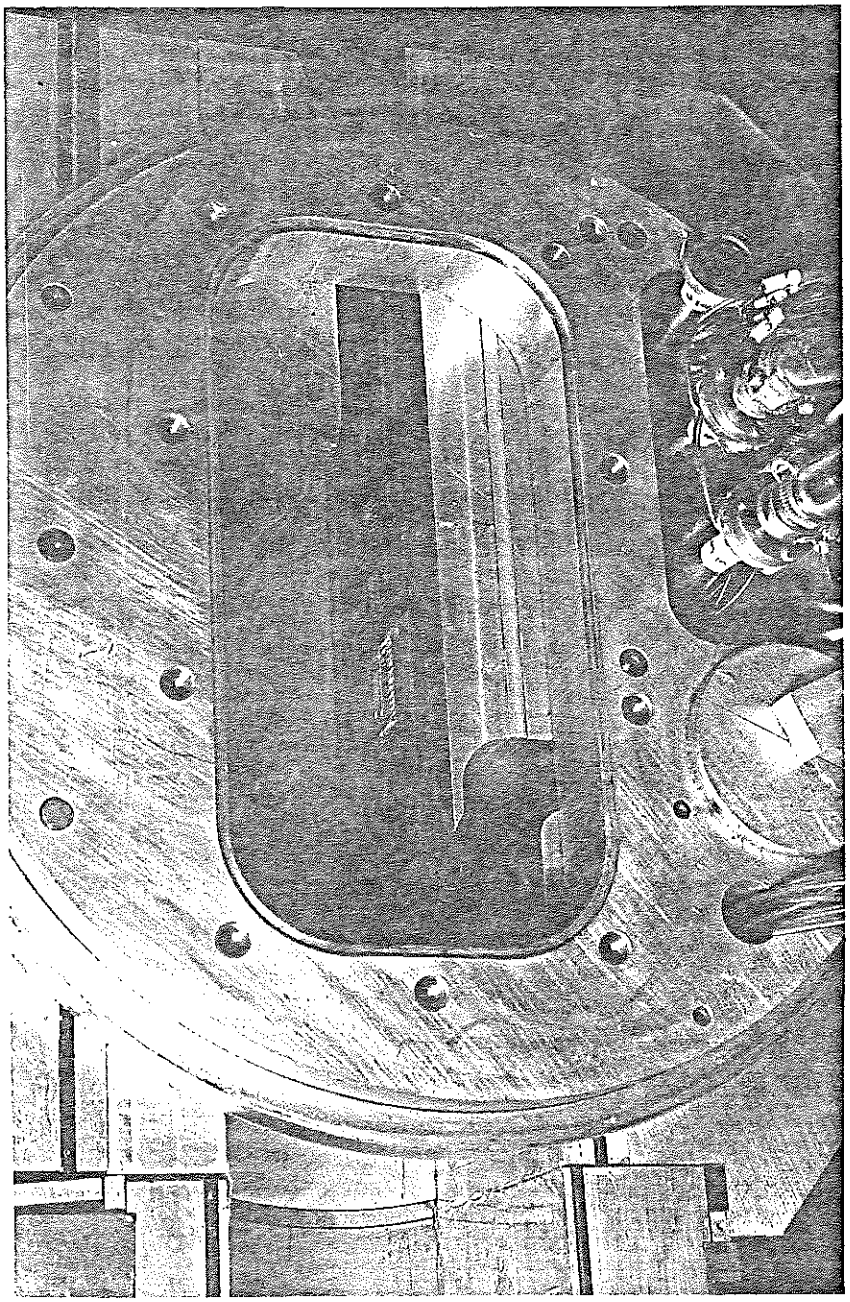

FIG.5.A

THE FILM COOLED FLAT PLATE

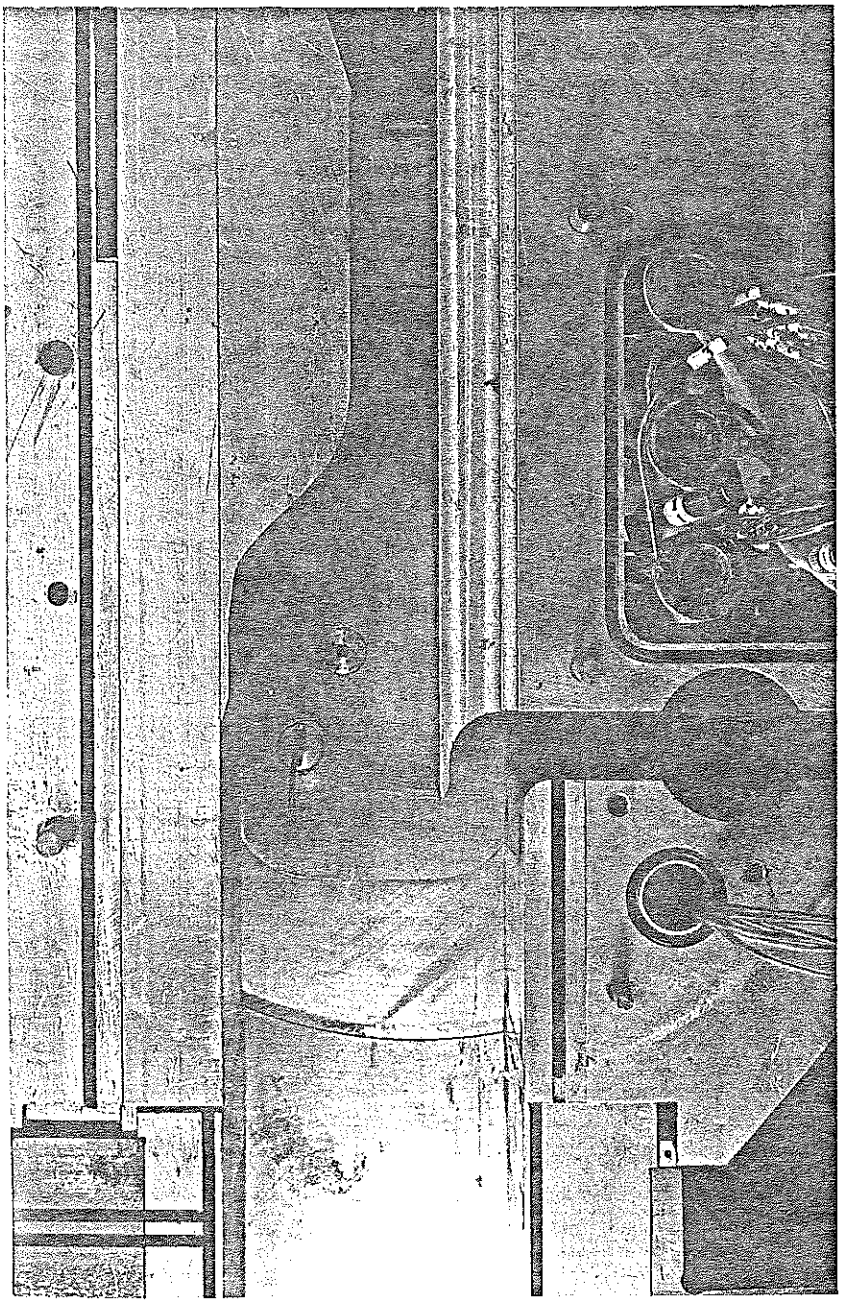

FIG.5.B
THE FILM COOLED FLAT PLATE

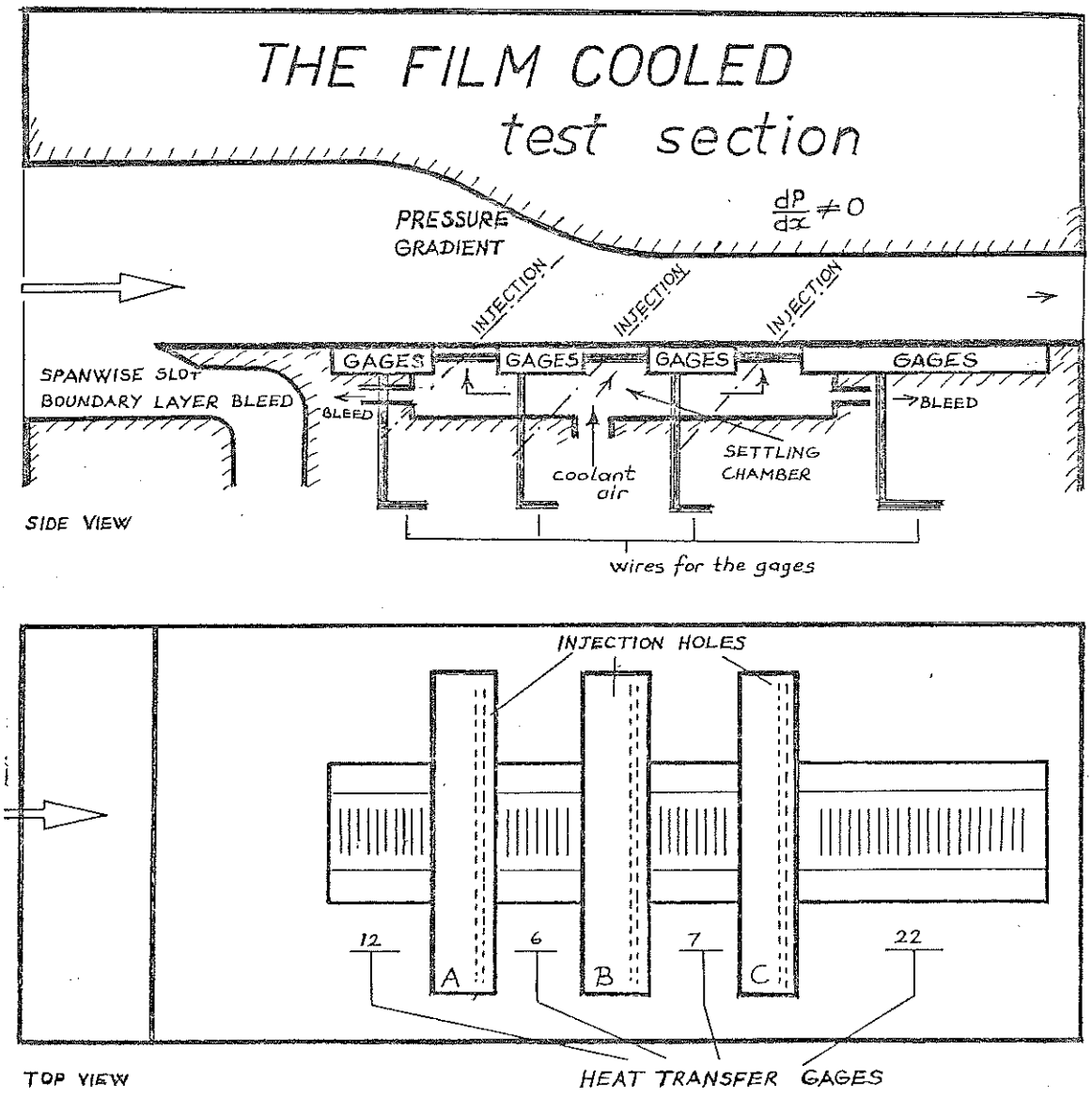
THE FILM COOLED
test section
$\frac{dP}{dx} \neq 0$
PRESSURE
GRADIENT
INJECTION
INJECTION
INJECTION
GAGES
GAGES
GAGES
GAGES
SPANWISE SLOT
BOUNDARY LAYER BLEED
BLEED
BLEED
SETTLING
CHAMBER
coolant
air
SIDE VIEW
wires for the gages
INJECTION HOLES
12
6
7
22
A
B
C
TOP VIEW
HEAT TRANSFER GAGES

FIG.6

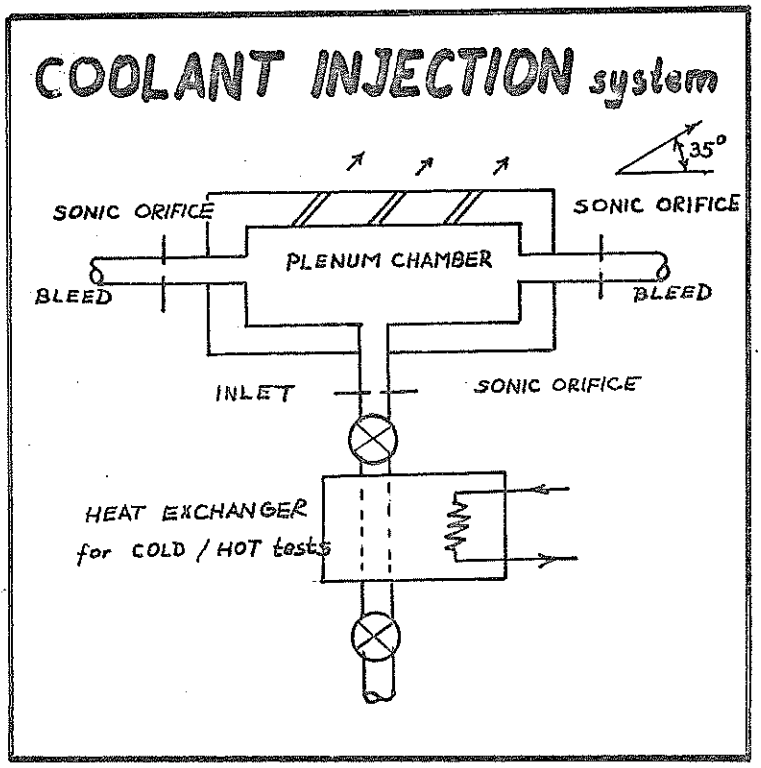
COOLANT INJECTION system
35°
SONIC ORIFICE
SONIC ORIFICE
PLENUM CHAMBER
BLEED
BLEED
INLET
SONIC ORIFICE
HEAT EXCHANGER
for COLD / HOT tests

FIG.7

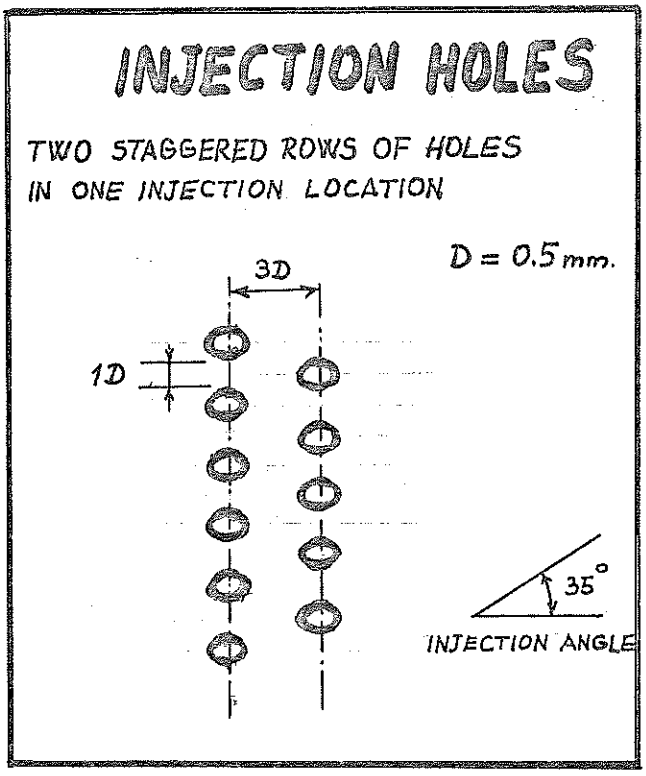
INJECTION HOLES
TWO STAGGERED ROWS OF HOLES
IN ONE INJECTION LOCATION
D = 0.5 mm.
3D
1D
35°
INJECTION ANGLE

FIG.8

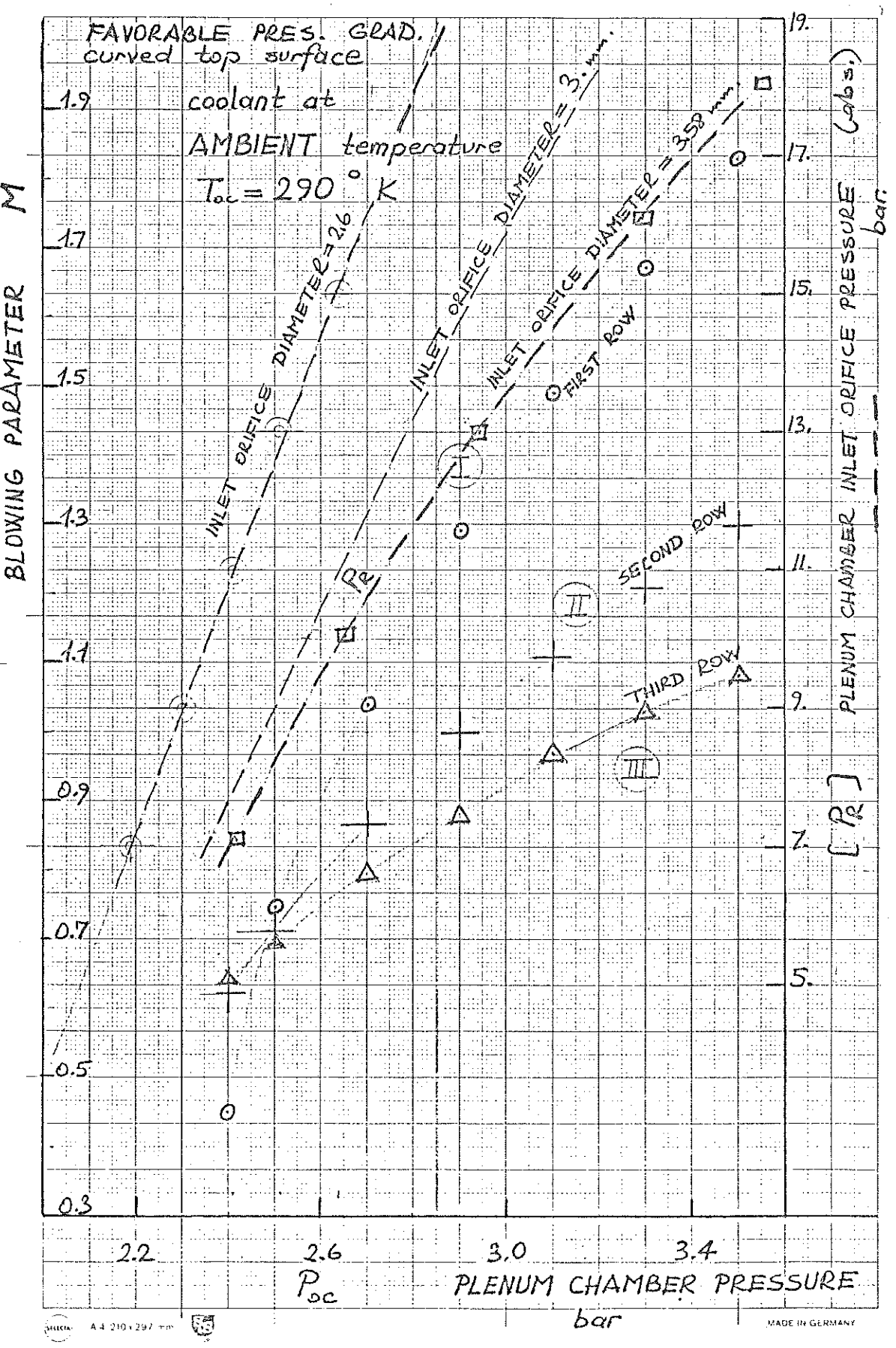
FAVORABLE PRES. GRAD.
curved top surface
coolant at
AMBIENT temperature
$T_{oc} = 290\ ^{\circ}K$
INLET ORIFICE DIAMETER = 2.6 mm.
INLET ORIFICE DIAMETER = 3.1 mm.
INLET ORIFICE DIAMETER = 3.58 mm.
FIRST ROW
SECOND ROW
THIRD ROW
I
II
III
Re
BLOWING PARAMETER M
PLENUM CHAMBER INLET ORIFICE PRESSURE [Re] (abs.) bar
1.9
1.7
1.5
1.3
1.1
0.9
0.7
0.5
0.3
19.
17.
15.
13.
11.
9.
7.
5.
2.2
2.6
3.0
3.4
P_{oc}
PLENUM CHAMBER PRESSURE
bar
A4 210 x 297 mm
MADE IN GERMANY

FIG.9

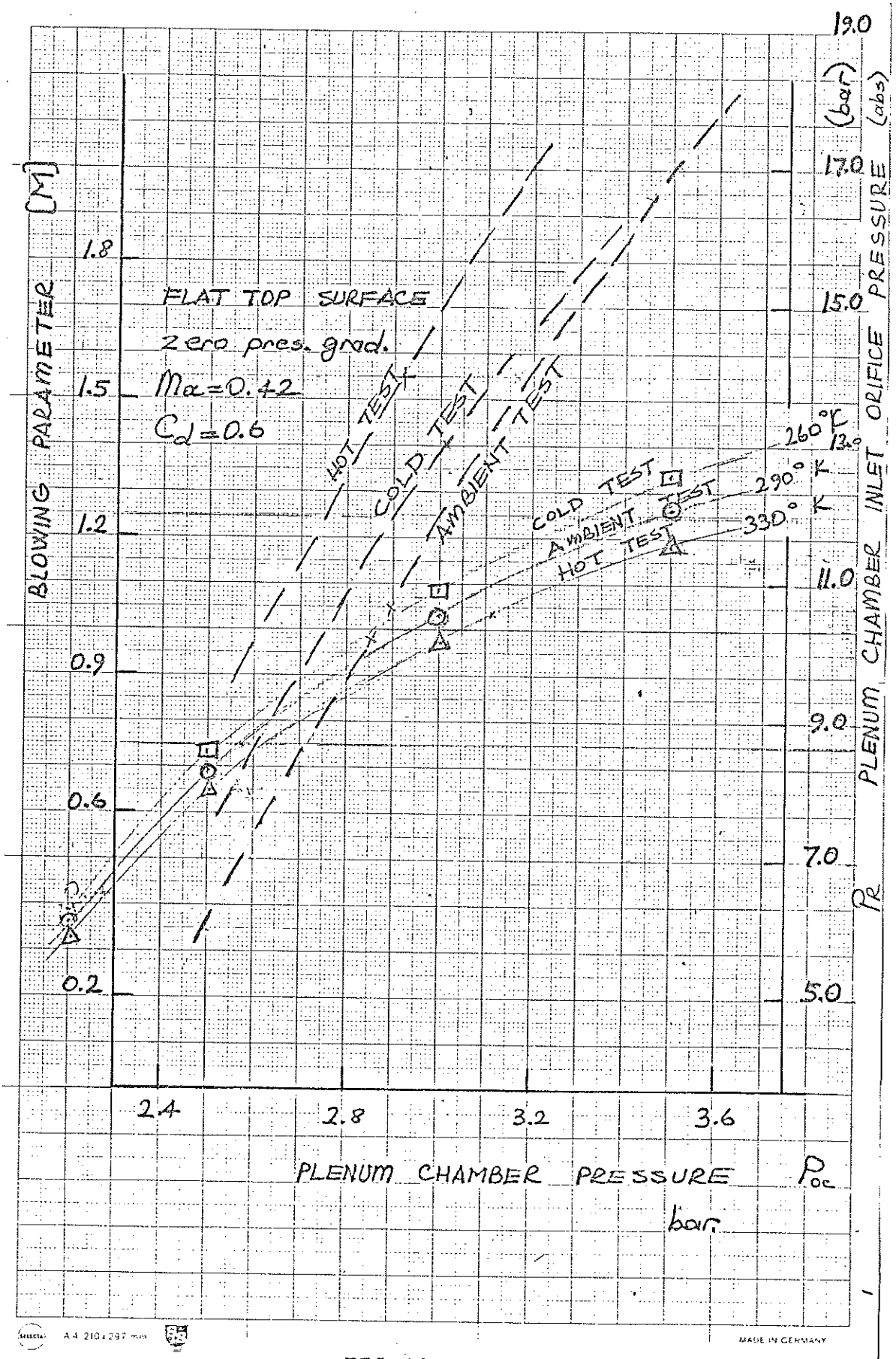
BLOWING PARAMETER [M]
1.8
1.5
1.2
0.9
0.6
0.2
FLAT TOP SURFACE
zero pres. grad.
$M_\infty = 0.42$
$C_d = 0.6$
HOT TEST
COLD TEST
AMBIENT TEST
260° K
290° K
330° K
2.4
2.8
3.2
3.6
PLENUM CHAMBER PRESSURE P_{oc}
bar
PLENUM CHAMBER INLET ORIFICE PRESSURE (abs)
19.0
17.0
15.0
13.0
11.0
9.0
7.0
5.0
(bar)
P_R

FIG. 10

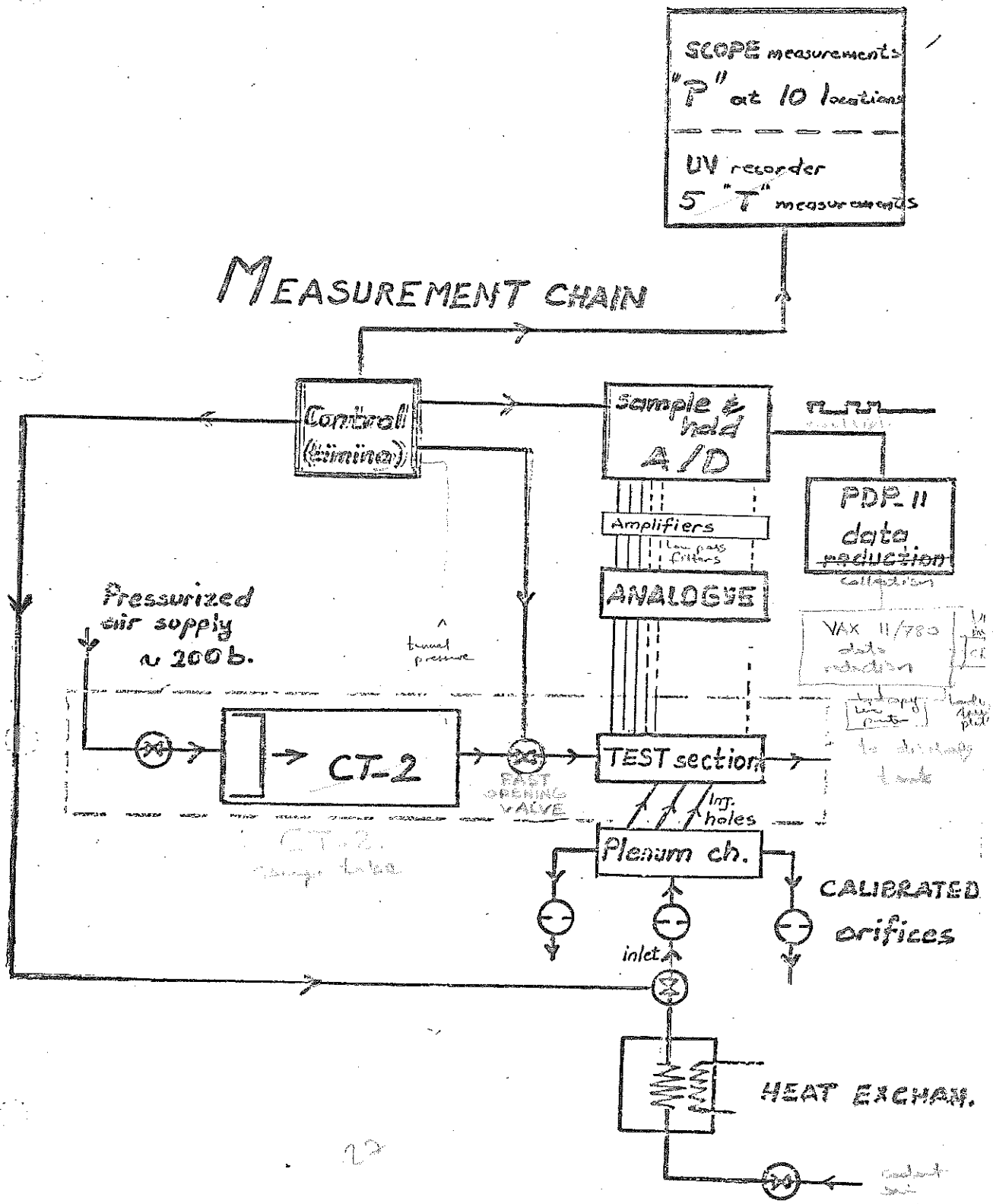
SCOPE measurements
"P" at 10 locations
UV recorder
5 "T" measurements
MEASUREMENT CHAIN
Control
(timing)
Sample & hold
A/D
PDP-11
data reduction
Amplifiers
Low pass filters
ANALOGUE
VAX 11/780
Pressurized air supply
~ 200 b.
CT-2
TEST section
Inj. holes
Plenum ch.
CALIBRATED orifices
inlet
HEAT EXCHAN.

FIG. 11

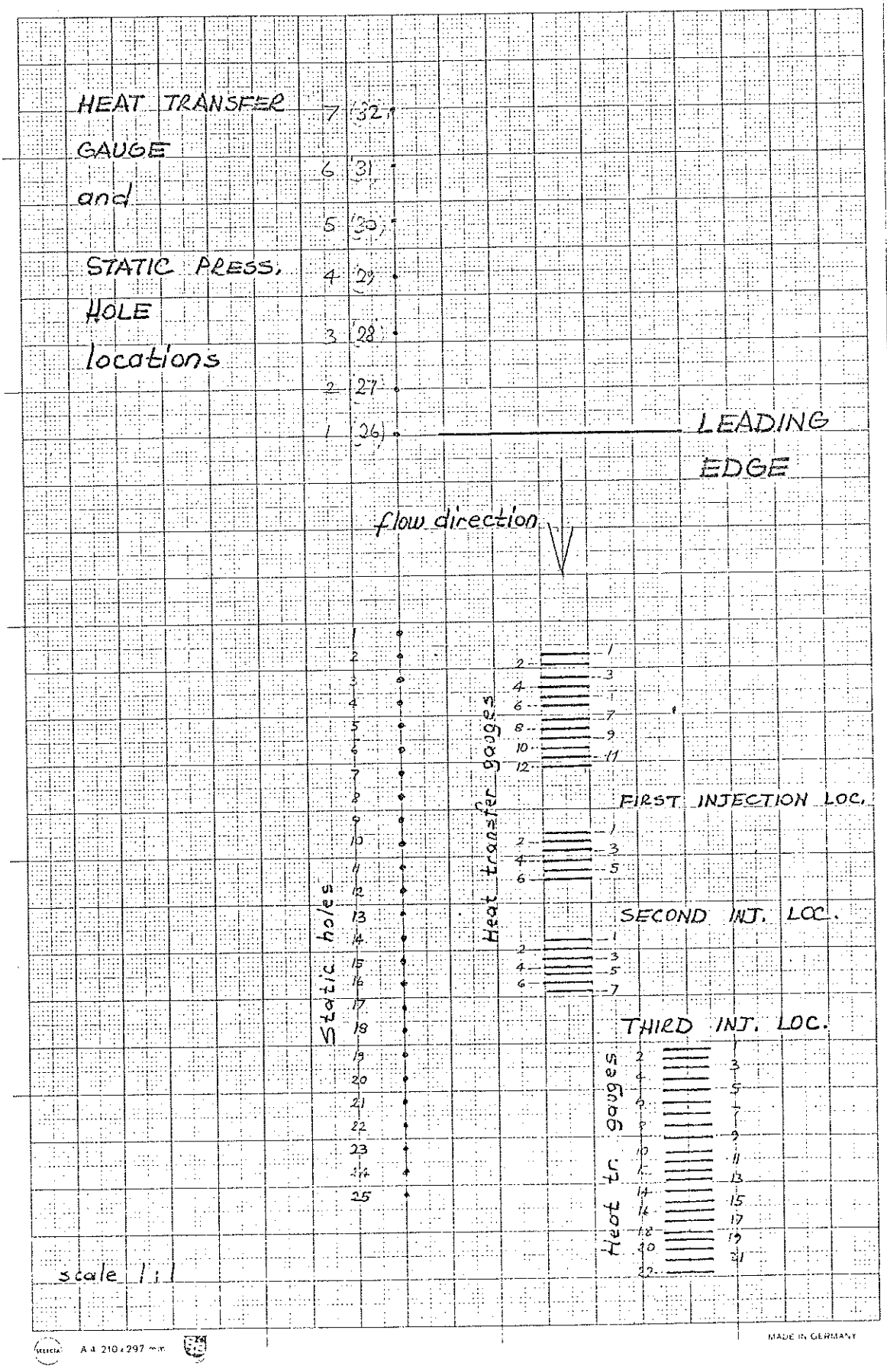
HEAT TRANSFER GAUGE and STATIC PRESS. HOLE locations
LEADING EDGE
flow direction
Static holes
Heat transfer gauges
FIRST INJECTION LOC.
SECOND INJ. LOC.
THIRD INJ. LOC.
Heat tr. gauges
scale 1:1
A4 210x297 mm
MADE IN GERMANY

FIG.12

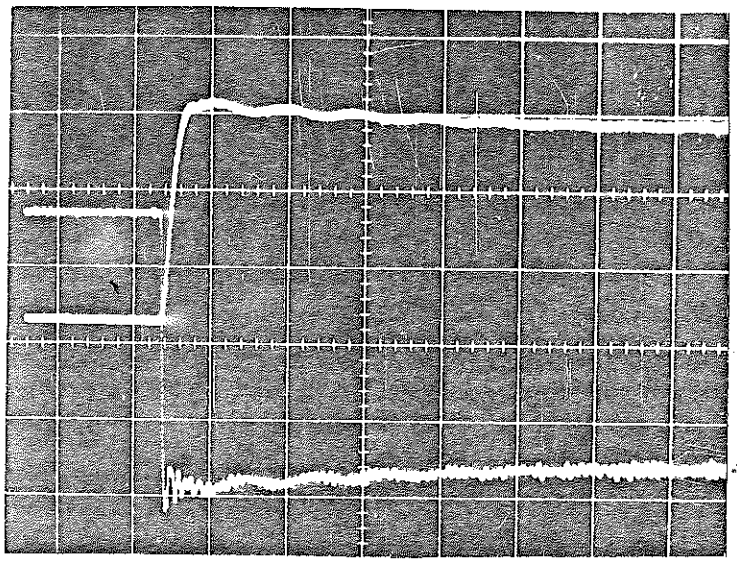

FREE STREAM TOTAL PRESSURE

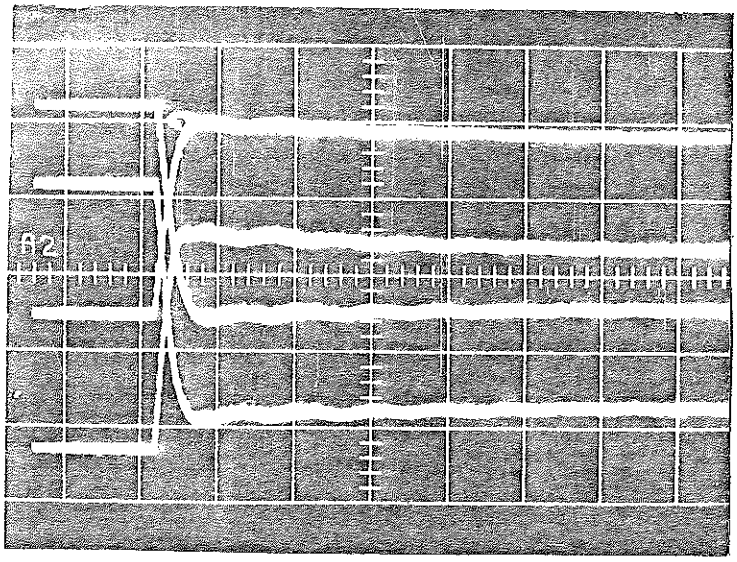

STATIC PRESSURES AT VARIOUS LOCATIONS ALONG THE FLAT PLATE

FIG. 13

PRESSURE TRACES

A TYPICAL TEMPERATURE TRACE

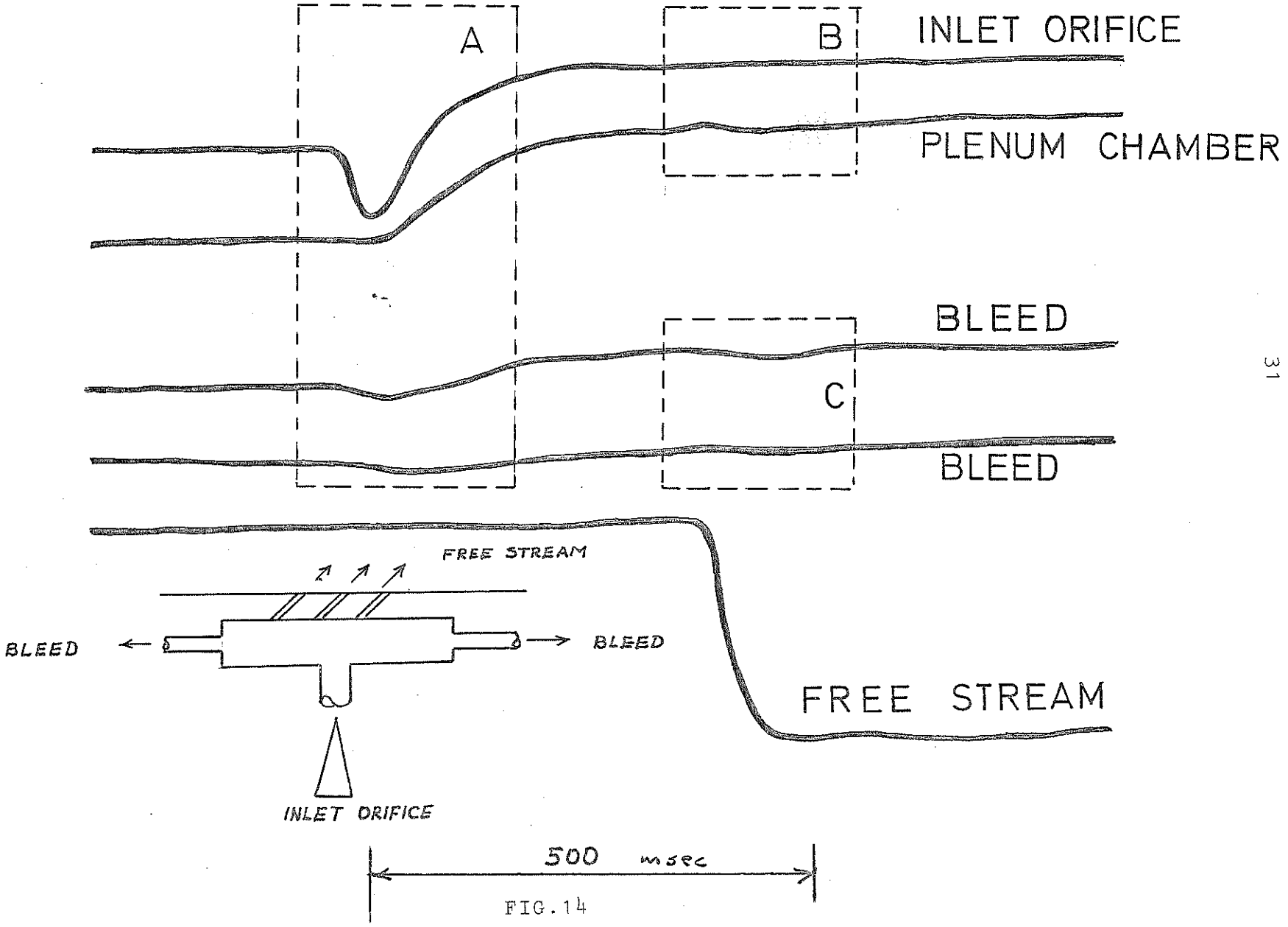

FIG. 14

HEAT TRANSFER MEASUREMENTS
analogue circuits

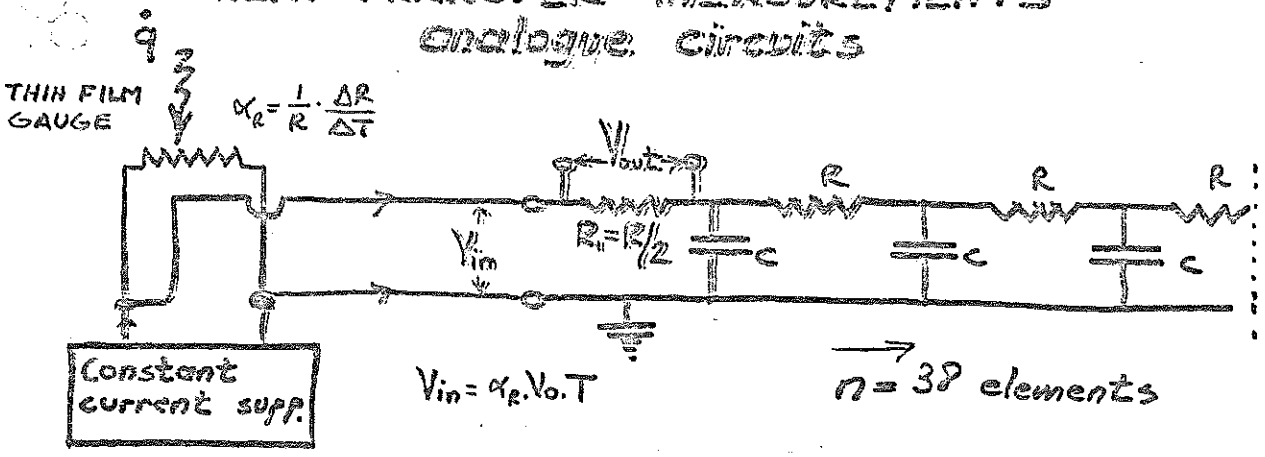

THE FLOW OF HEAT INTO THE SEMIINFINITE MATERIAL

(1) $\frac{\partial \dot{q}}{\partial x} = \rho c \frac{\partial T}{\partial t}$

$-\dot{q} = k \frac{\partial T}{\partial x}$

THE CURRENT FLOW INTO A MEDIUM CONTAINING DISTRIBUTED R and C

$\frac{\partial i}{\partial x} = c' \frac{\partial V}{\partial t}$ (2)

$-i = \frac{1}{r'} \frac{\partial V}{\partial x}$

ANALOGOUS quantities

$\dot{q} \equiv i \qquad T \equiv V \qquad k = \frac{1}{r'} \qquad \rho c = \frac{1}{c'}$

using Laplace transforms + $t = 0 \quad T = V = 0$

$\dot{q} = \sqrt{\rho c k} . \sqrt{p} . T$

$x = \infty \quad T = V = 0$

$i = \sqrt{\frac{c'}{r'}} . \sqrt{p} . V$

$Y = \alpha_R . V_0 . T$

$i = \sqrt{\frac{c'}{r'}} \sqrt{p} . \alpha_R . V_0 . T$

$i = \frac{V_{out}}{R_1}$

$$\dot{q}(t) = \sqrt{\rho c k} . \sqrt{\frac{r'}{c'}} . \frac{1}{\alpha_R . V_0} . \frac{V_{out}}{R_1}$$

FIG. 15

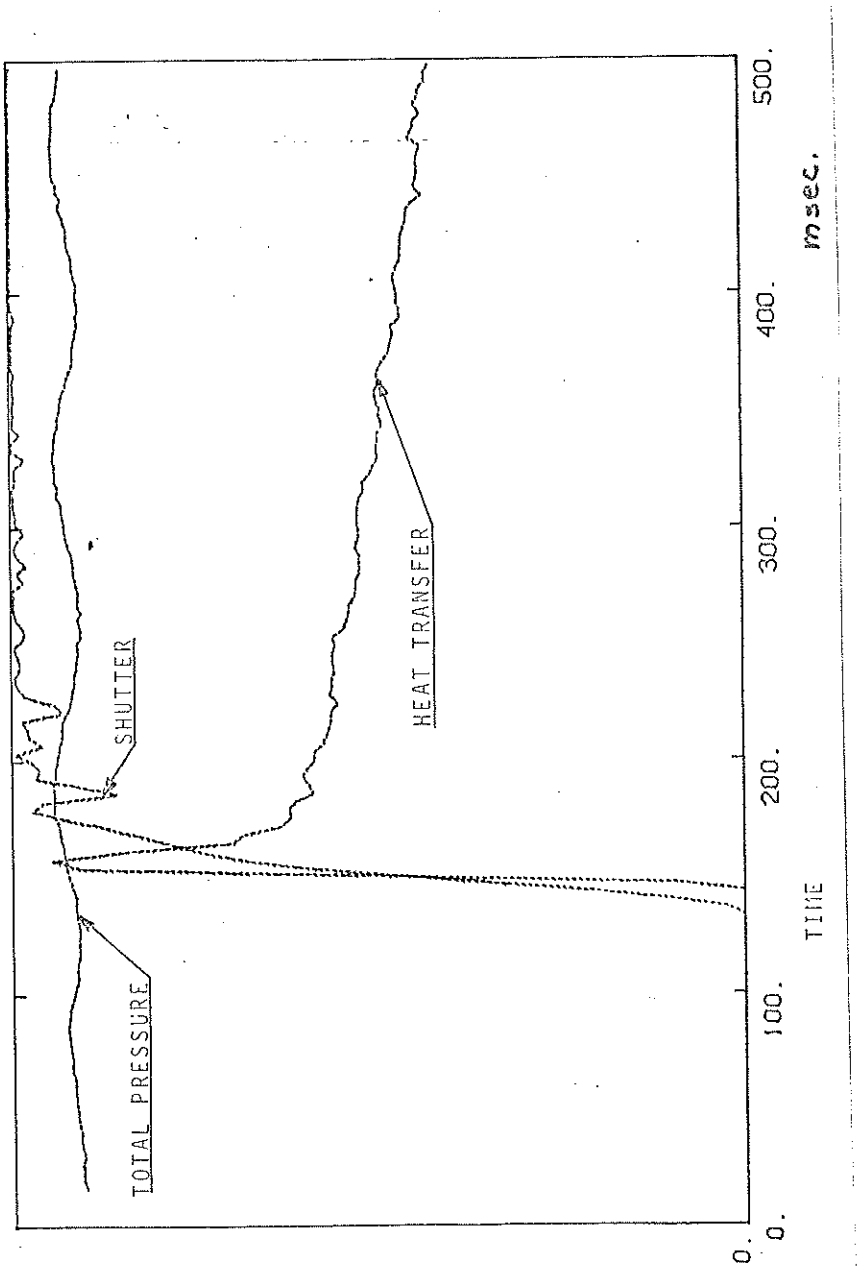

FIG. 16

FREE STREAM TOTAL PRESSURE, HEAT TRANSFER AND SHUTTER SIGNAL

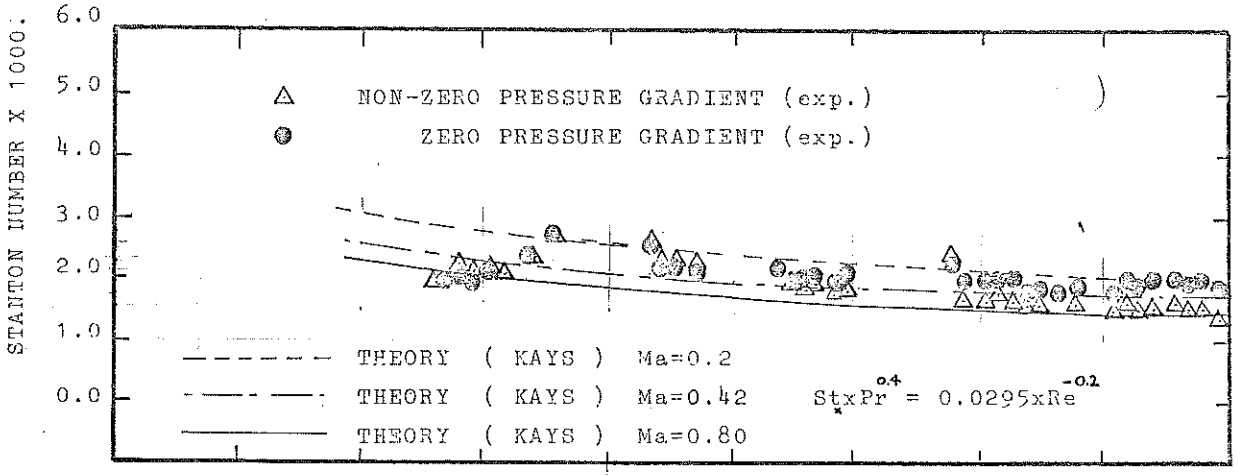

STANTON NUMBER DISTRIBUTION OVER THE FLAT PLATE / without injection

FIG.17

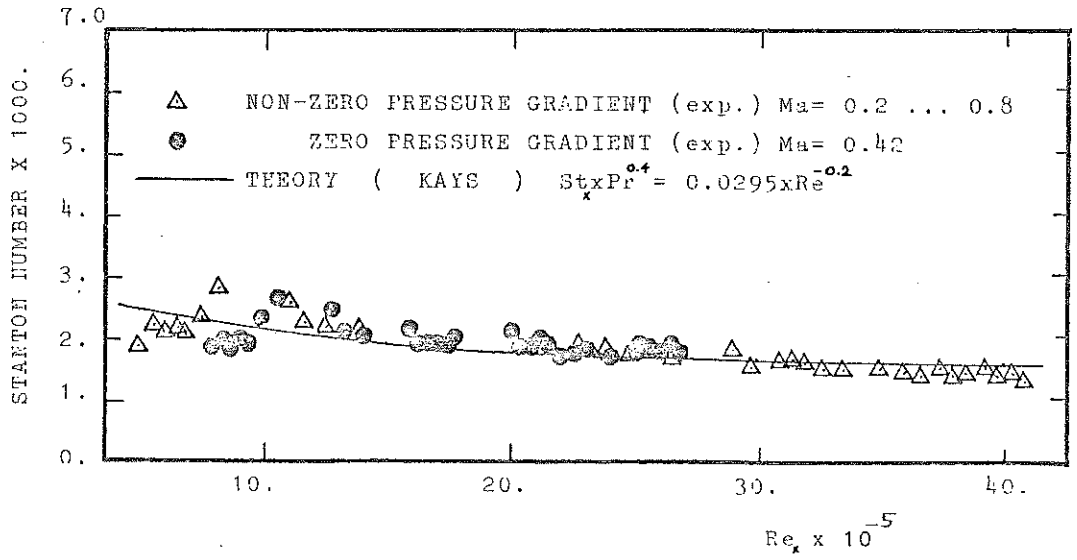

STANTON NUMBER DISTRIBUTION OVER THE FLAT PLATE
(without injection)

FIG.18

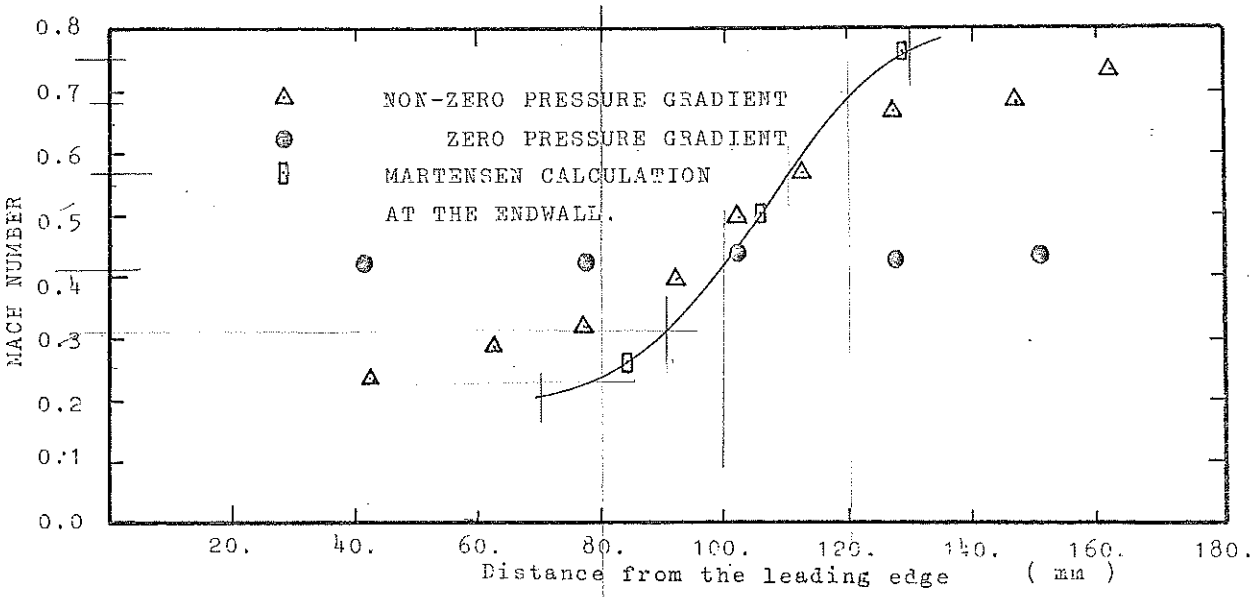

MACH NUMBER DISTRIBUTION OVER THE FLAT PLATE

FIG.19

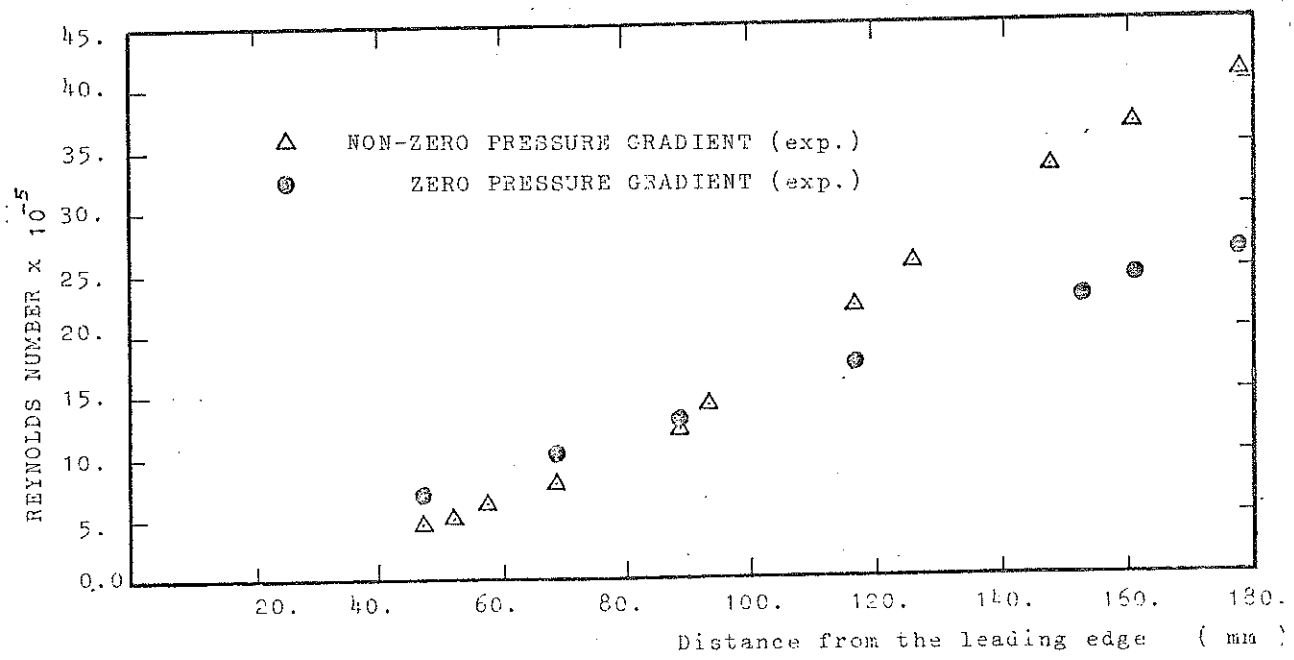

REYNOLDS NUMBER DISTRIBUTION OVER THE FLAT PLATE
(From static pressure measurements)

FIG.20

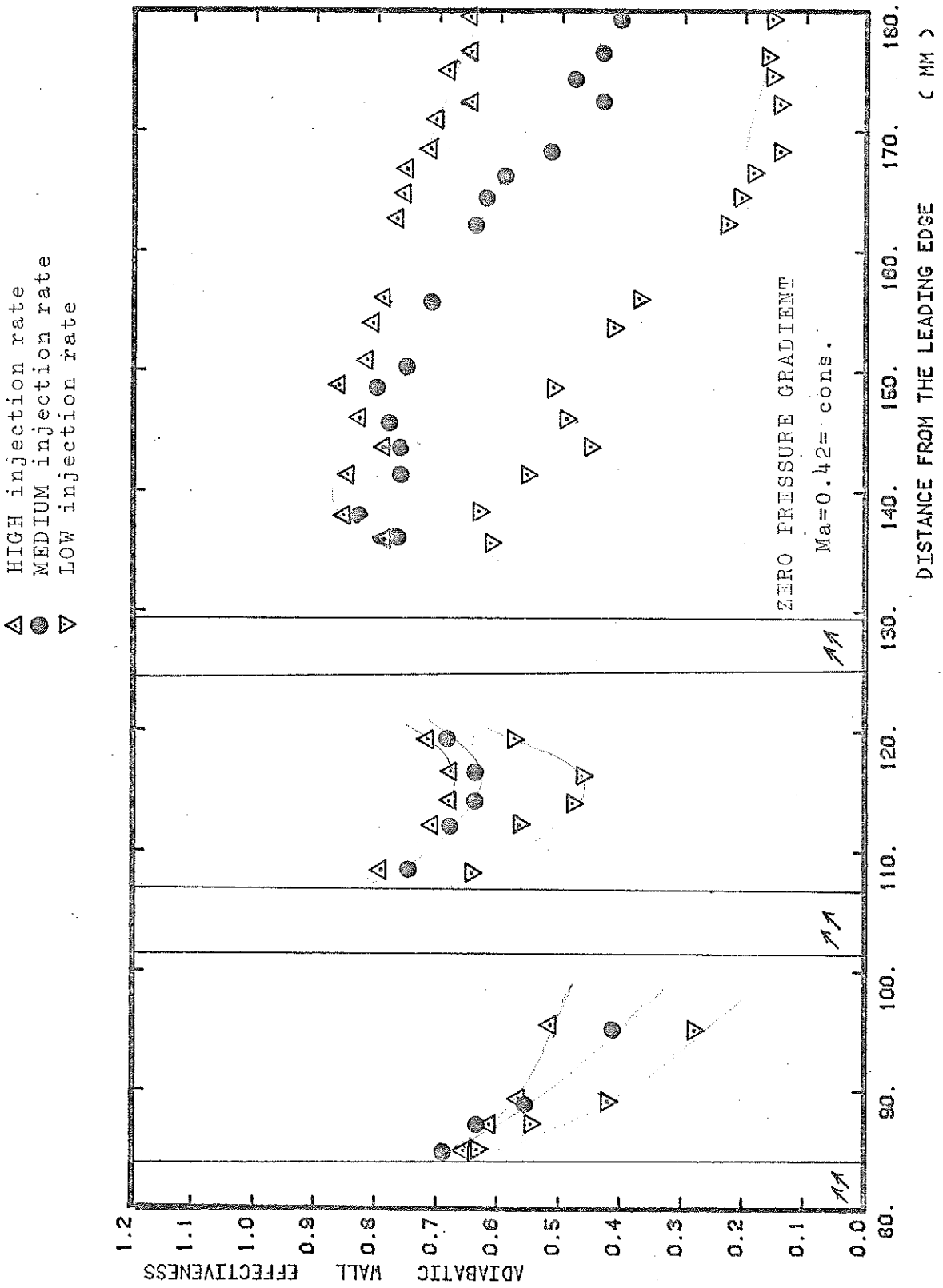

ADIABATIC WALL EFFECTIVENESS DISTRIBUTION OVER THE FLAT PLATE

+ FIG.21

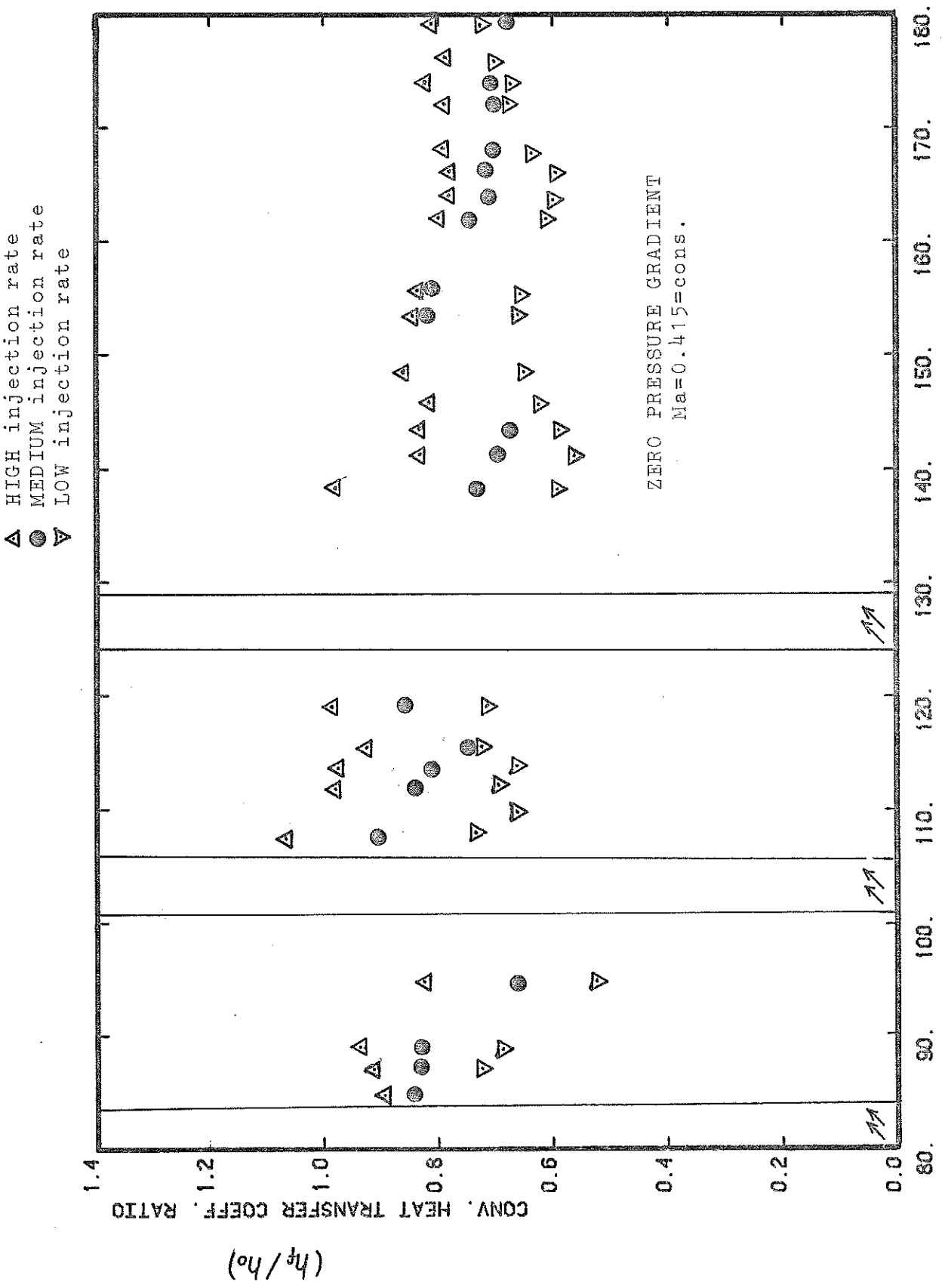

HEAT TRANSFER COEFF. RATIO DISTRIBUTION (h_f/h_o)

FIG.22

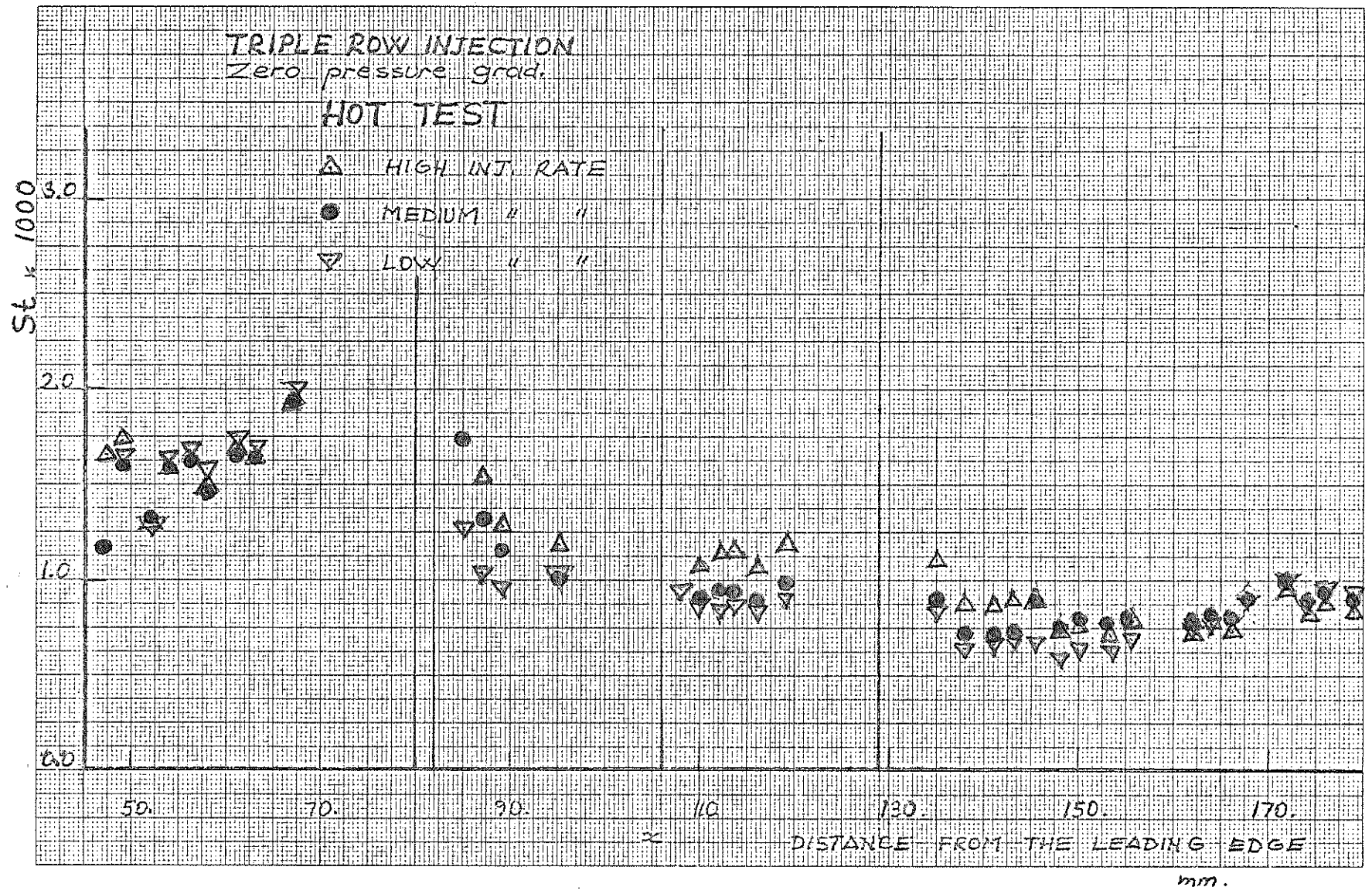
TRIPLE ROW INJECTION
Zero pressure grad.
HOT TEST
HIGH INJ. RATE
MEDIUM " "
LOW " "
St x 1000
3.0
2.0
1.0
0.0
50.
70.
90.
110
130.
150.
170.
x
DISTANCE FROM THE LEADING EDGE
mm.

FIG.23

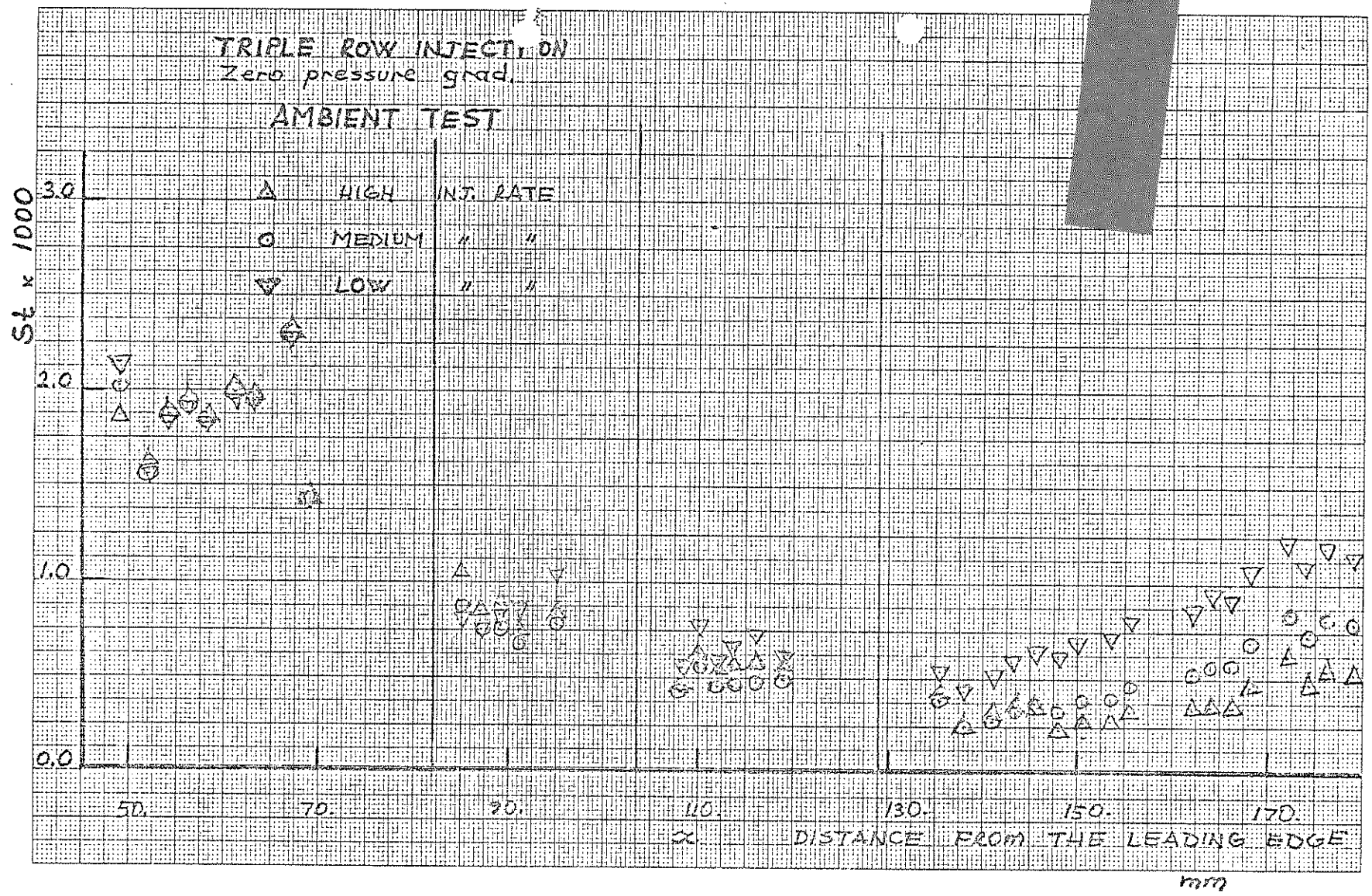
TRIPLE ROW INJECTION
Zero pressure grad.
AMBIENT TEST
HIGH INJ. RATE
MEDIUM " "
LOW " "
St x 1000
3.0
2.0
1.0
0.0
50.
70.
90.
110.
130.
150.
170.
x.
DISTANCE FROM THE LEADING EDGE
mm

FIG.24

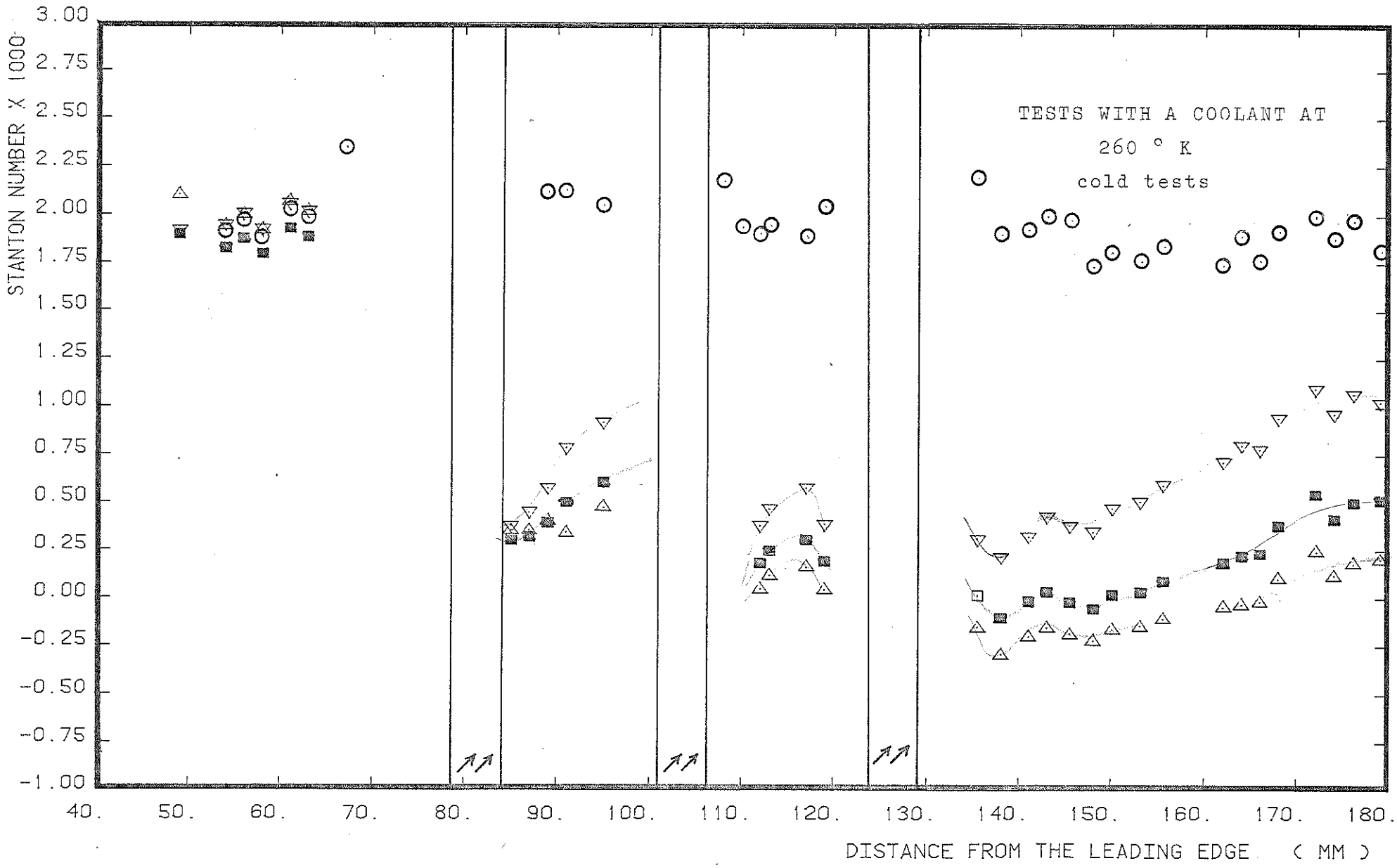

STANTON NUM. DISTR. (ZERO PRESS. GRAD. / COOLANT AT 260° K)

- ○ NO INJECTION
- ↗↗ INJECTION LOCATION
- △ HIGH INJECTION RATE
- ■ MEDIUM INJECTION RATE
- ▽ LOW INJECTION RATE

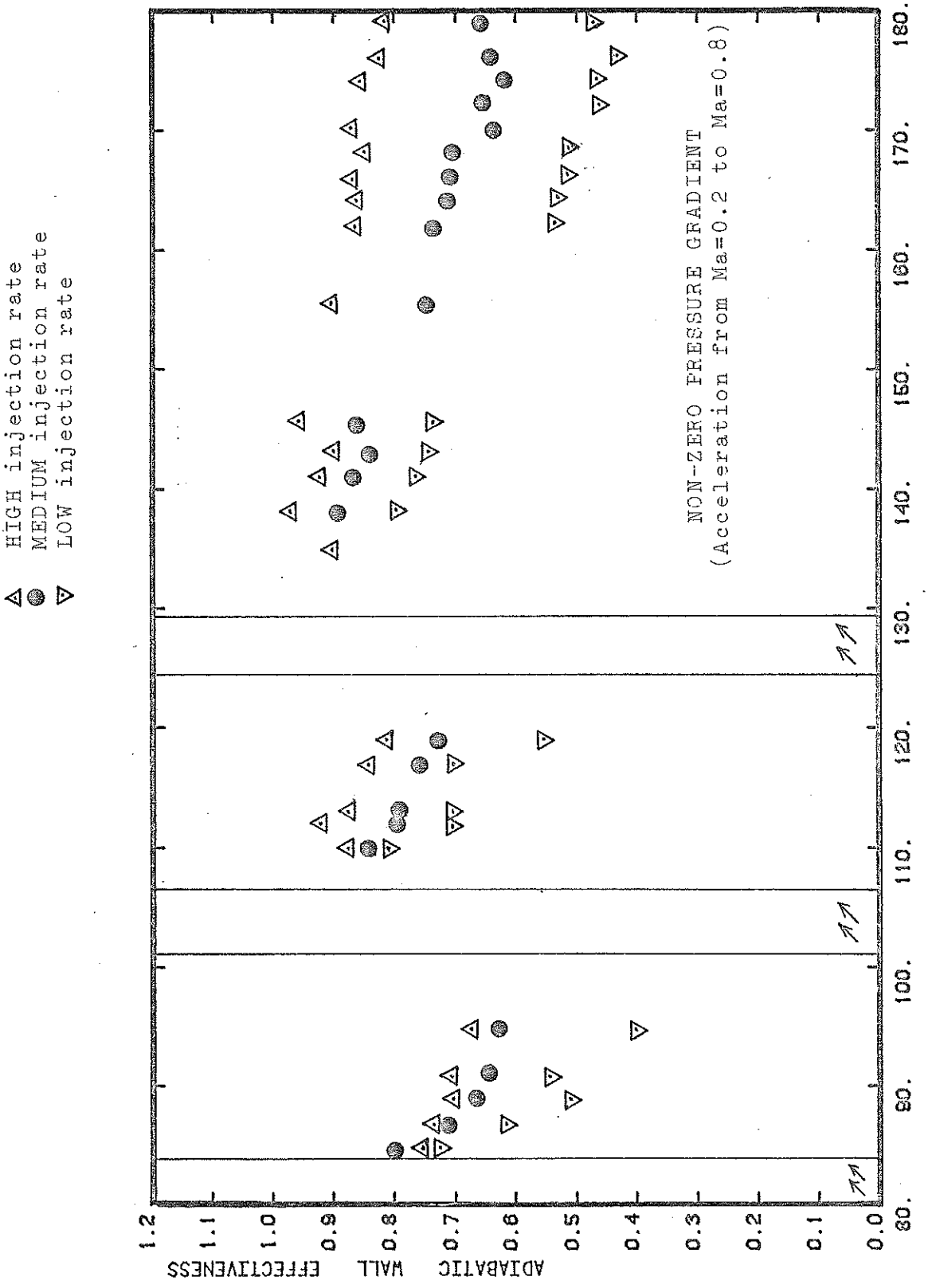

ADIABATIC WALL EFFECTIVENESS DISTRIBUTION OVER THE FLAT PLATE

FIG.26

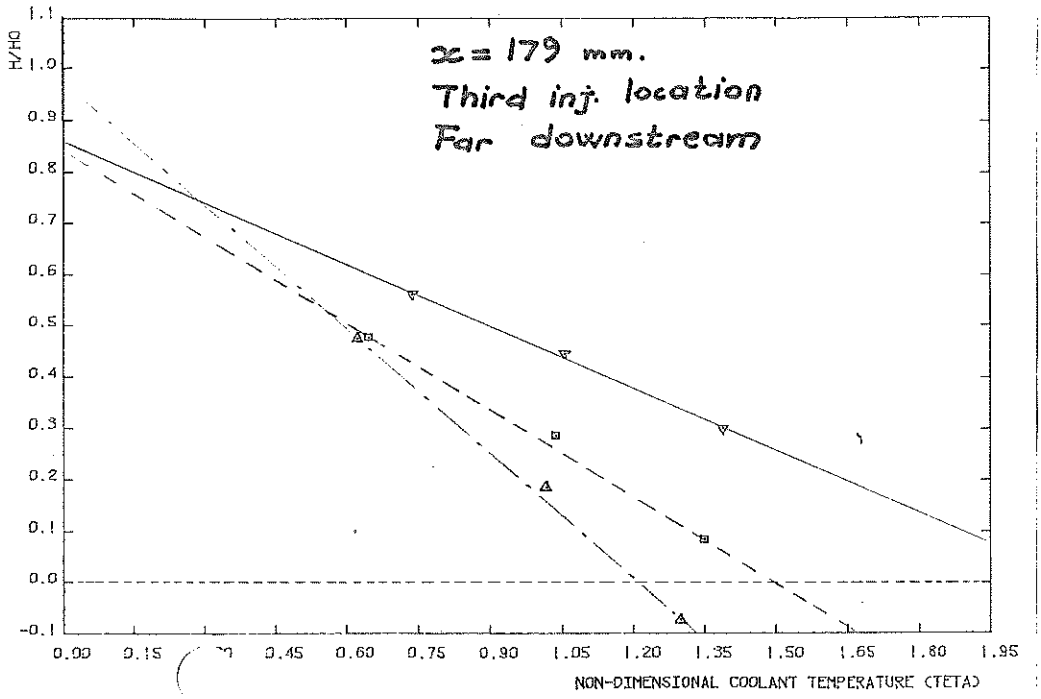

GRAPHICAL DETERMINATION OF ADIABATIC WALL EFFICIENCY

FIG.27

LINEAR RELATION BETWEEN h/h_o AND Θ

(EXPERIMENTAL POINTS) FAR DOWNSTREAM

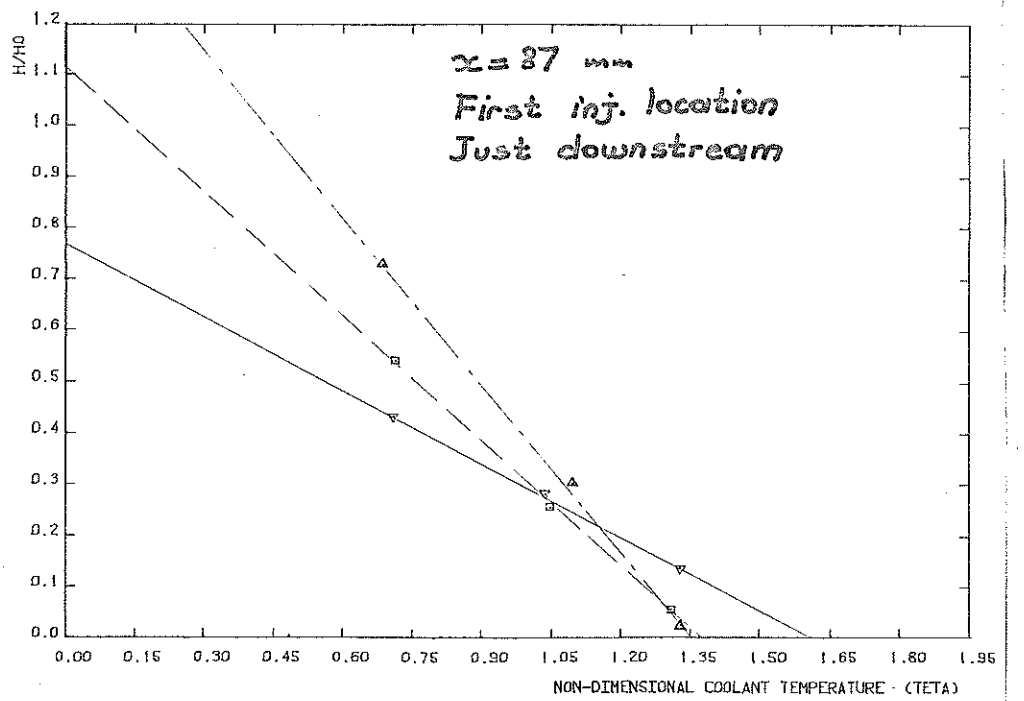

GRAPHICAL DETERMINATION OF ADIABATIC WALL EFFICIENCY

FIG.28

LINEAR RELATION BETWEEN h/h_o AND Θ

(EXPERIMENTAL POINTS) JUST DOWNSTREAM

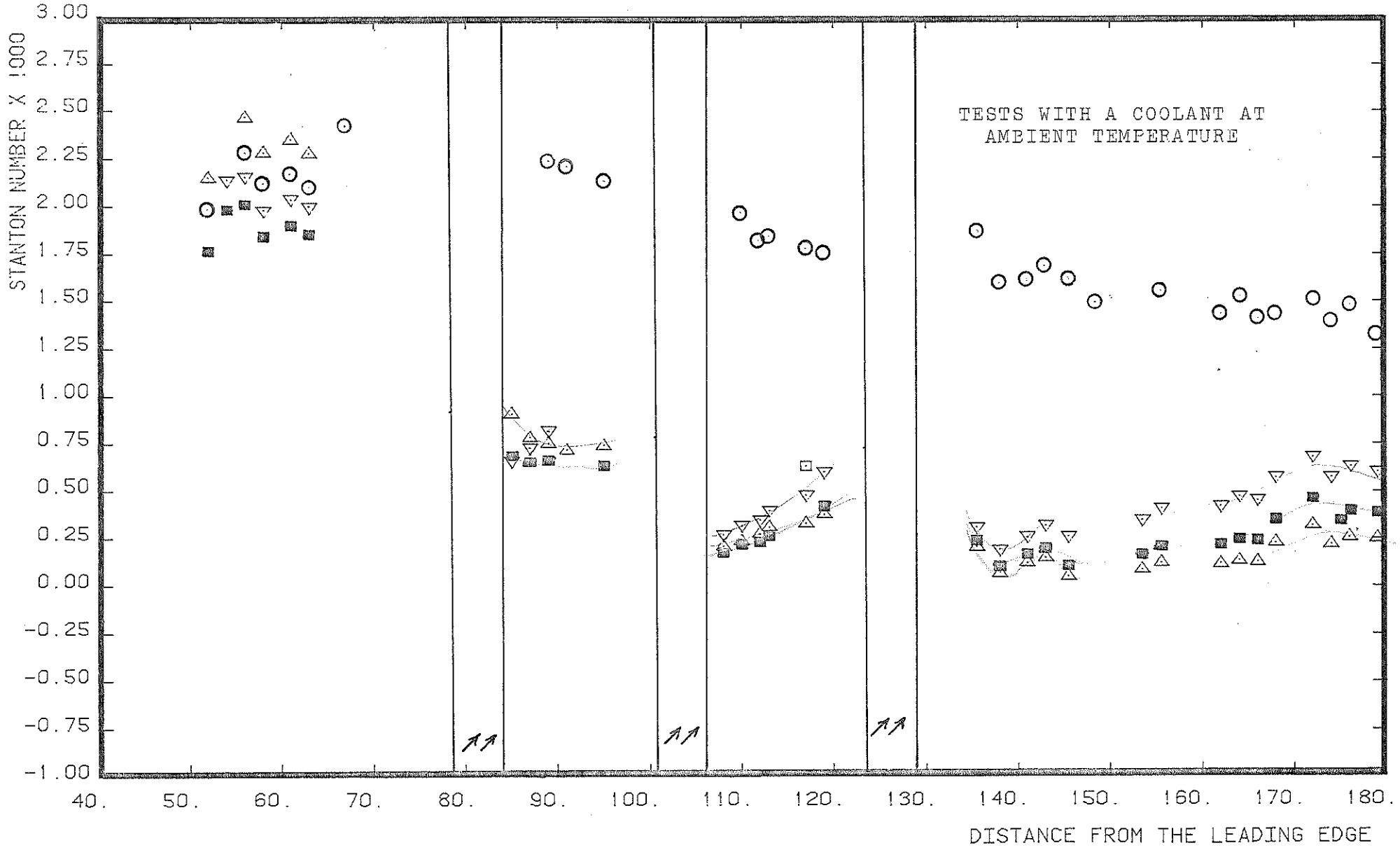

STANTON NUM. DISTR. (WITH PRESSURE GRADIENT/COOLANT AT AMBIENT TEMP.)

- ○ NO INJECTION
- ↗↗ INJECTION LOCATION
- △ HIGH INJECTION RATE
- ■ MEDIUM INJECTION RATE
- ▽ LOW INJECTION RATE

FIG.29

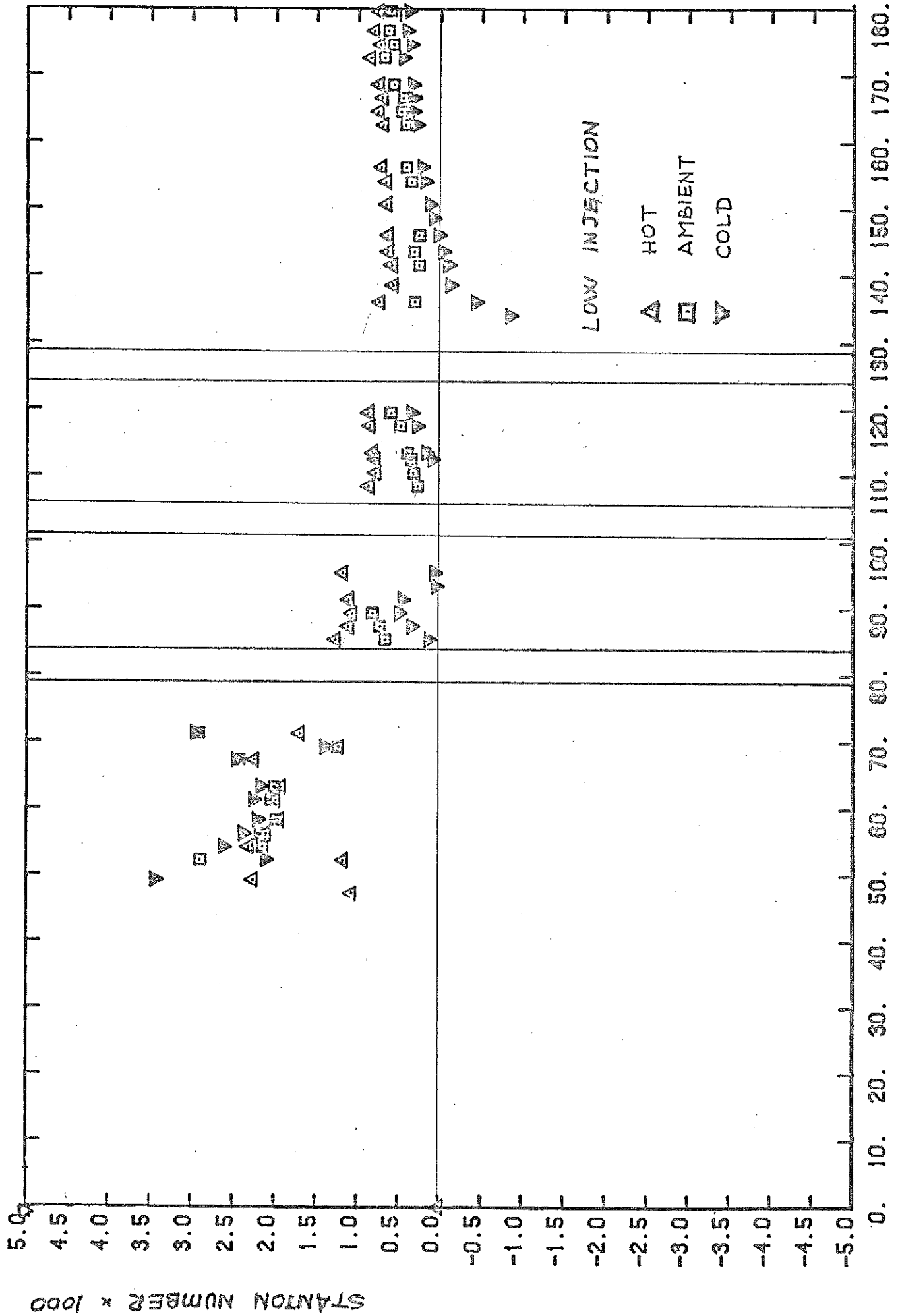
STANTON NUMBER × 1000
5.0
4.5
4.0
3.5
3.0
2.5
2.0
1.5
1.0
0.5
0.0
-0.5
-1.0
-1.5
-2.0
-2.5
-3.0
-3.5
-4.0
-4.5
-5.0
0.
10.
20.
30.
40.
50.
60.
70.
80.
90.
100.
110.
120.
130.
140.
150.
160.
170.
180.
x DISTANCE FROM THE LEADING EDGE (MM)
LOW INJECTION
HOT
AMBIENT
COLD

FIG.30

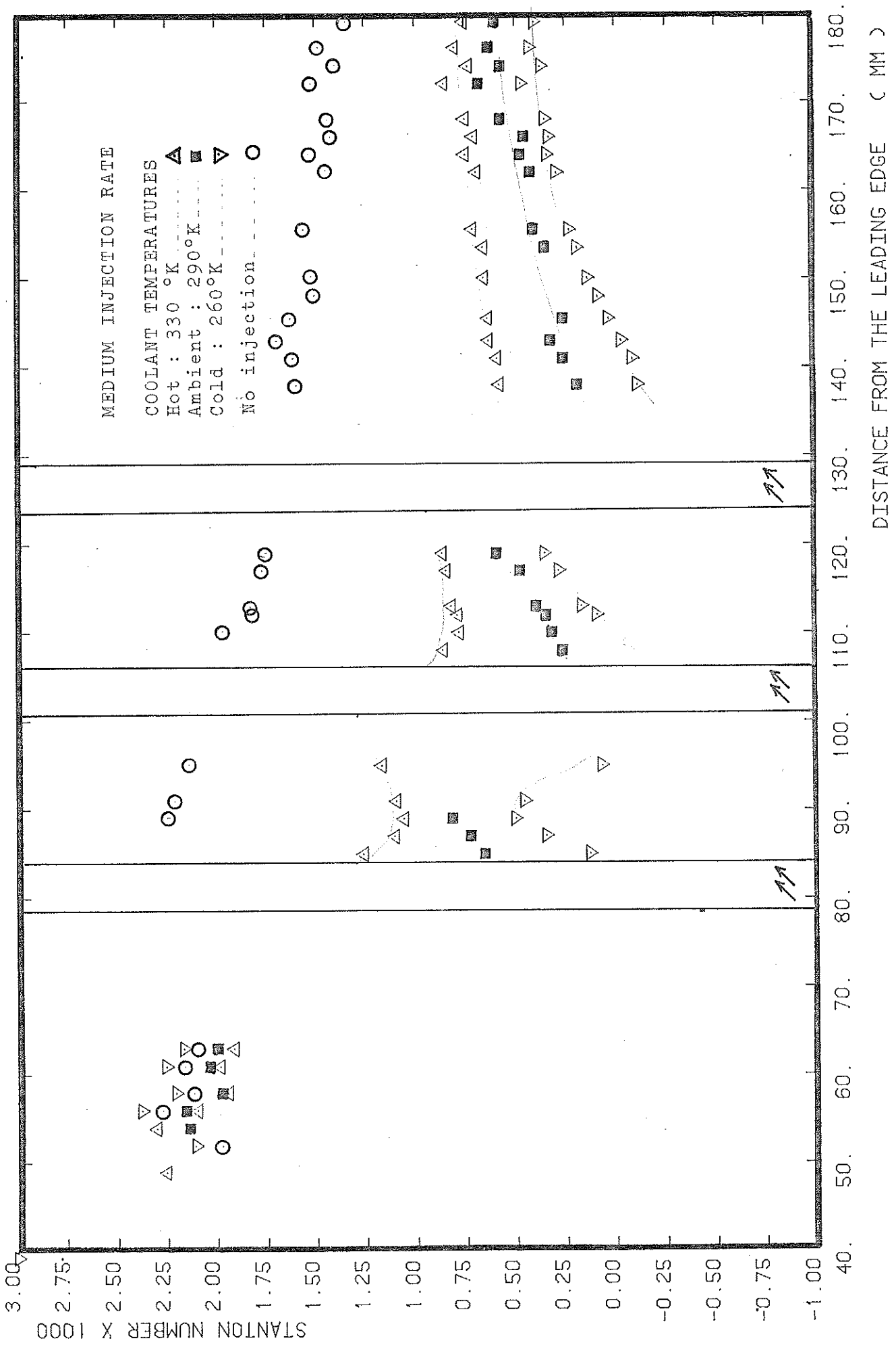

ST. NUMBER DISTR. (WITH PRESS. GRAD. / MEDIUM Injection)

FIG.31

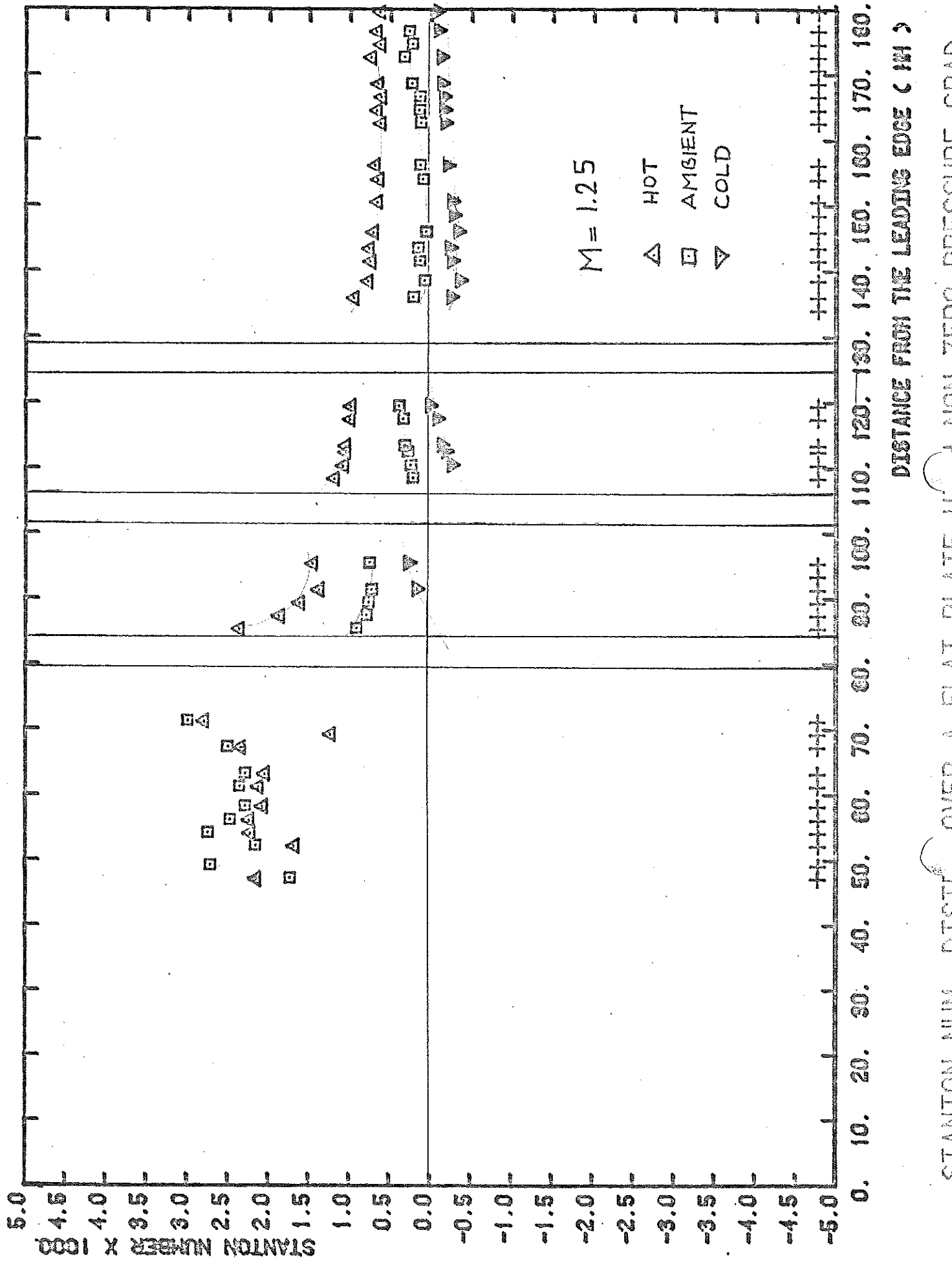

STANTON NUMBER DISTRIBUTION OVER A FLAT PLATE IN A NON-ZERO PRESSURE GRAD

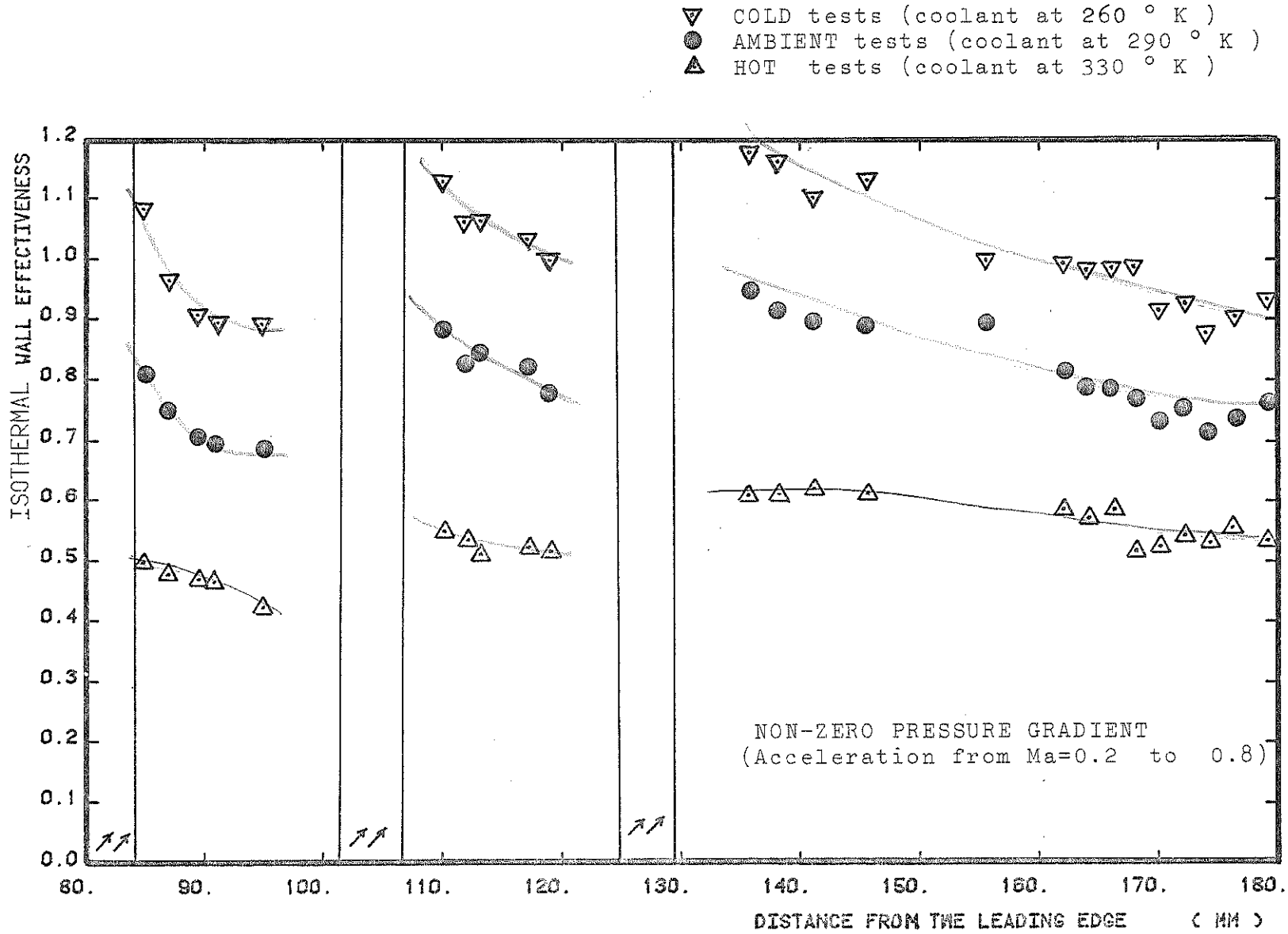

ISOTHERMAL WALL EFFECTIVENESS DISTRIBUTION

FIG 22

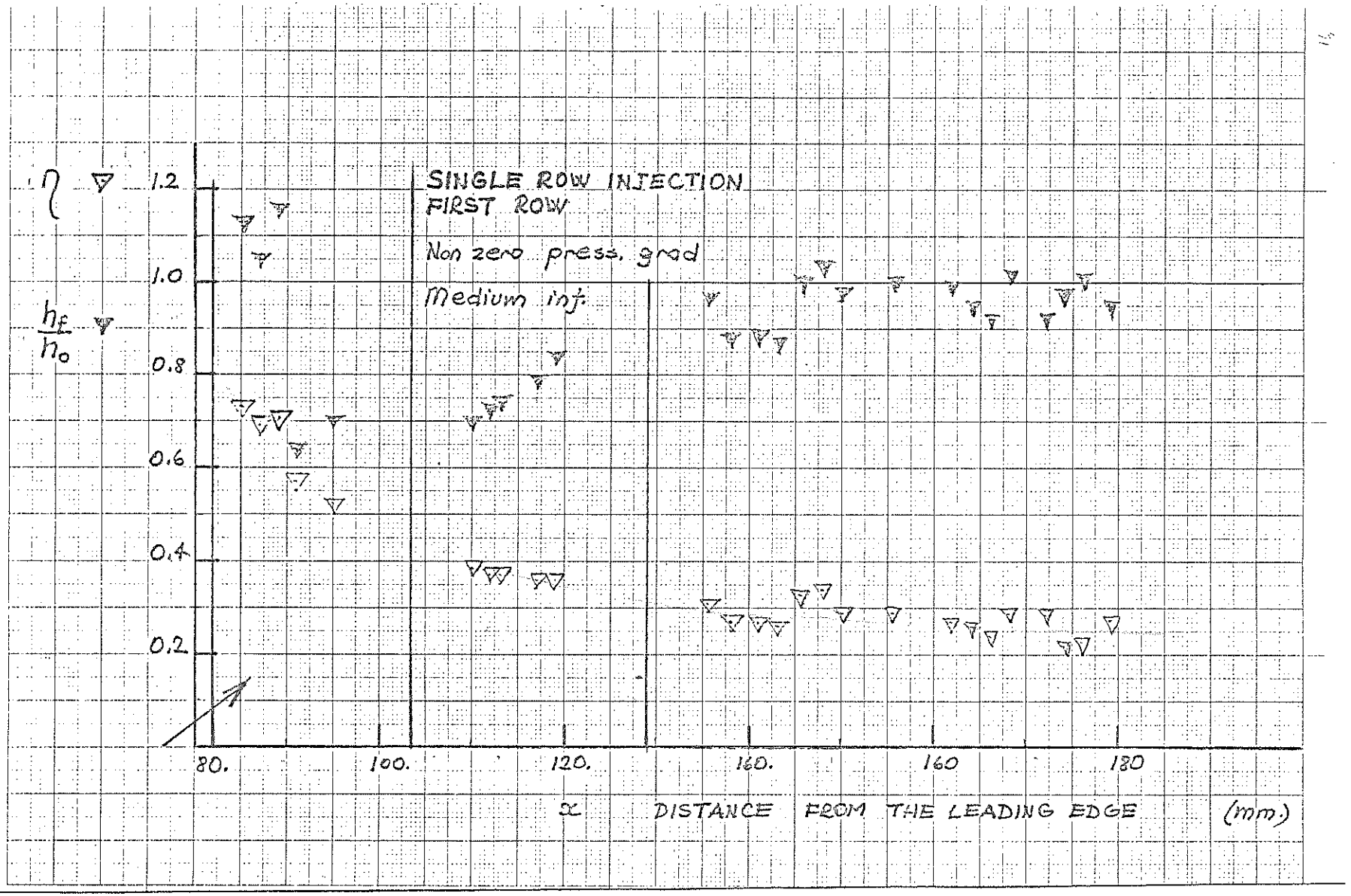
η
$\frac{h_f}{h_o}$
1.2
1.0
0.8
0.6
0.4
0.2
SINGLE ROW INJECTION
FIRST ROW
Non zero press. grad
Medium inj.
80.
100.
120.
160.
160
180
x DISTANCE FROM THE LEADING EDGE (mm.)

FIG. 31

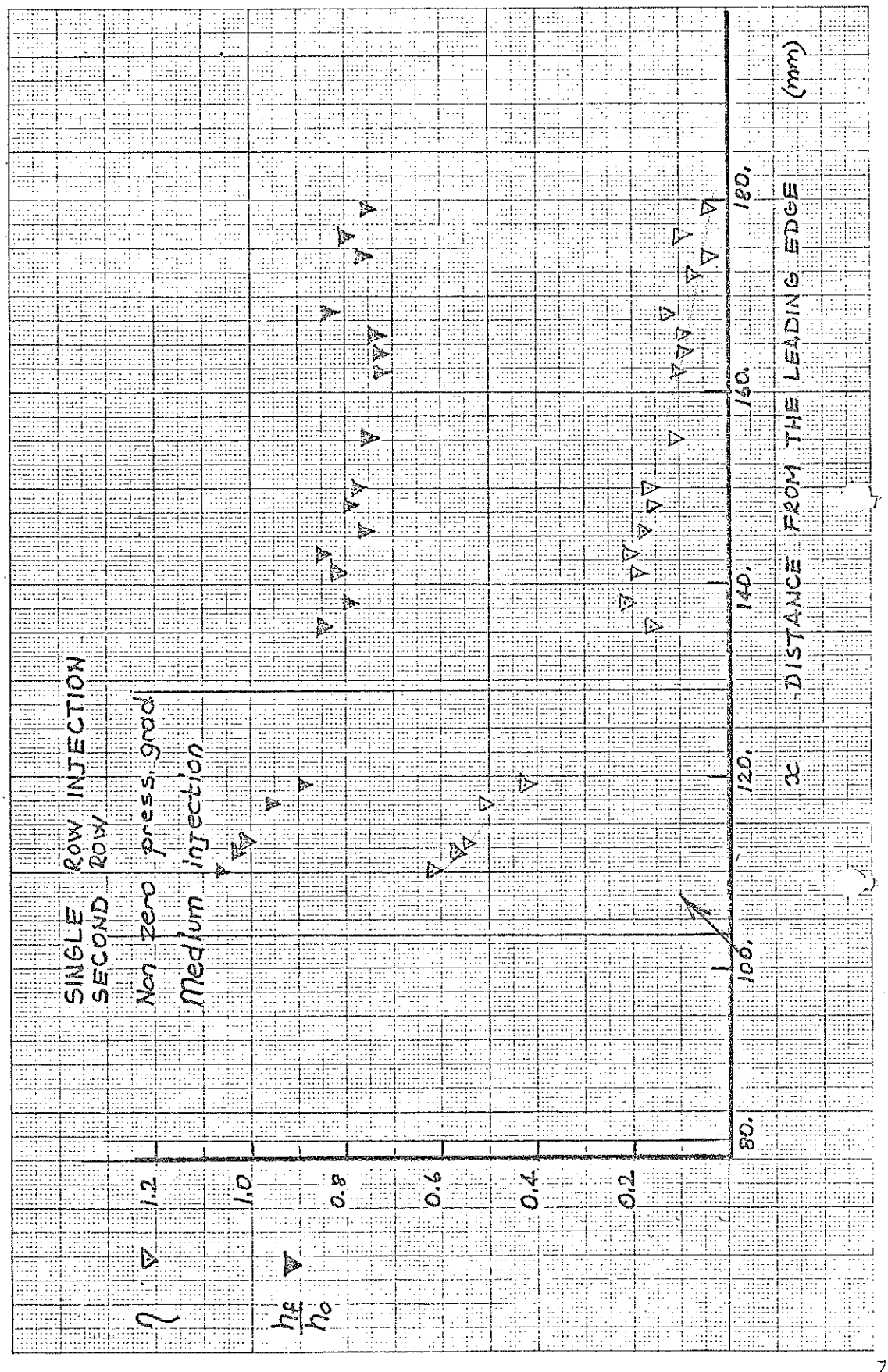
SINGLE ROW INJECTION
SECOND ROW
Non zero press. grad
Medium injection
$\frac{u}{u_0}$
1.2
1.0
0.8
0.6
0.4
0.2
80.
100.
120.
140.
160.
180.
x DISTANCE FROM THE LEADING EDGE (mm)

FIG.35

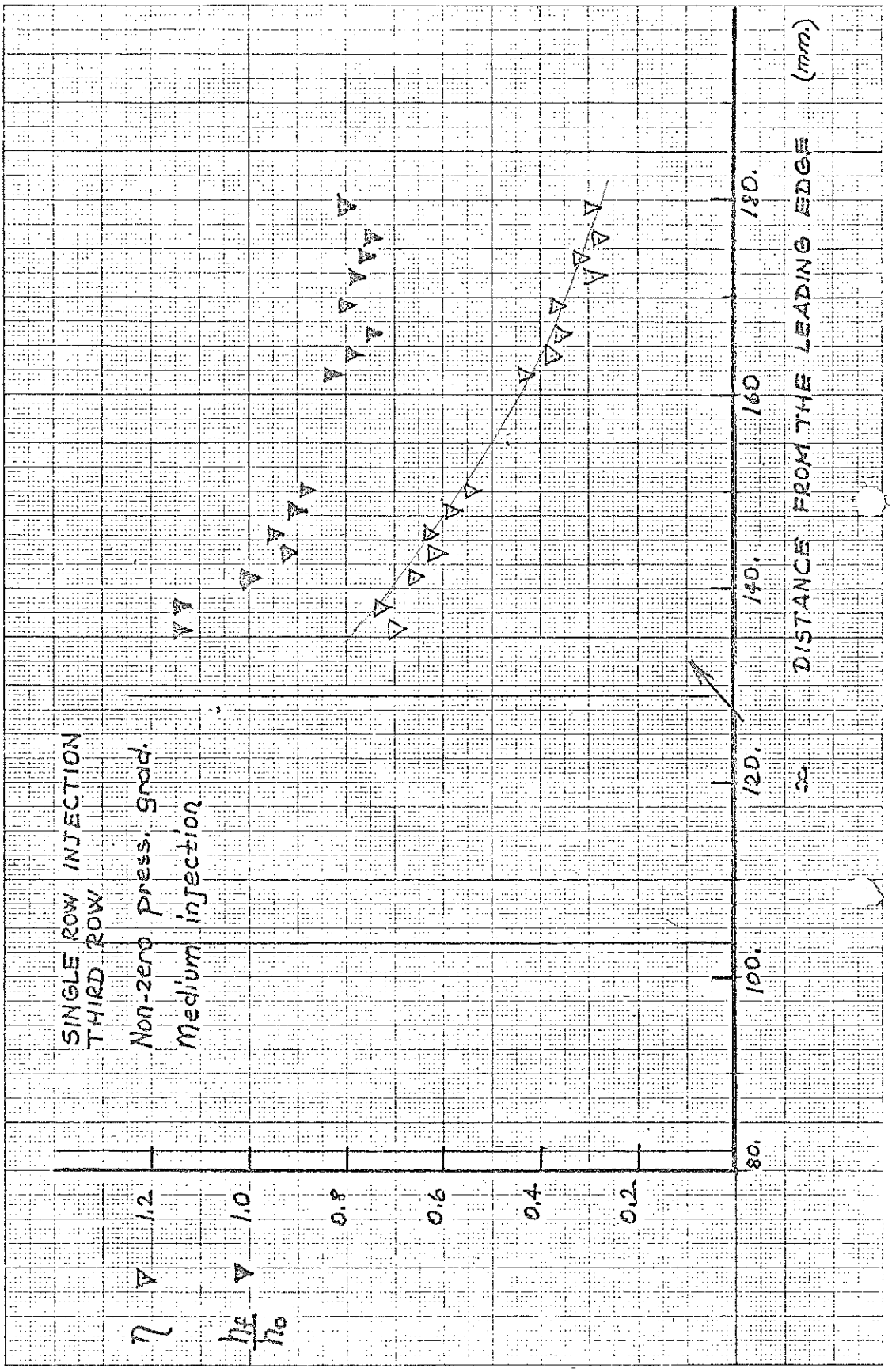
SINGLE ROW INJECTION
THIRD ROW
Non-zero Press. grad.
Medium injection
η
hs/ho
1.2
1.0
0.8
0.6
0.4
0.2
80.
100.
120.
140.
160
180.
DISTANCE FROM THE LEADING EDGE (mm.)

FIG. 36

SELLERS FILM SUPERPOSITION HYPOTHESIS

SINGLE ROW INJECTION

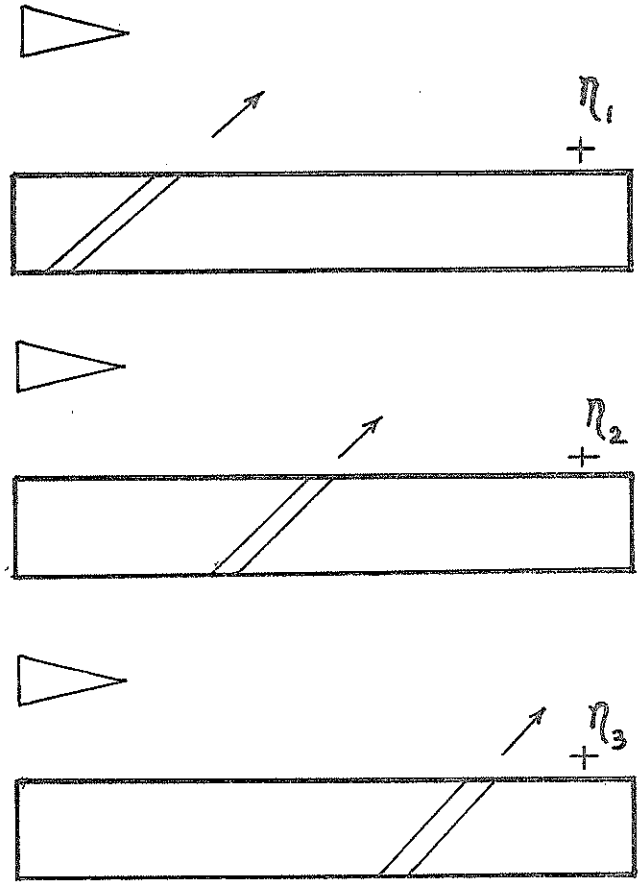

SELLERS' SUPERPOSITION HYPOTHESIS

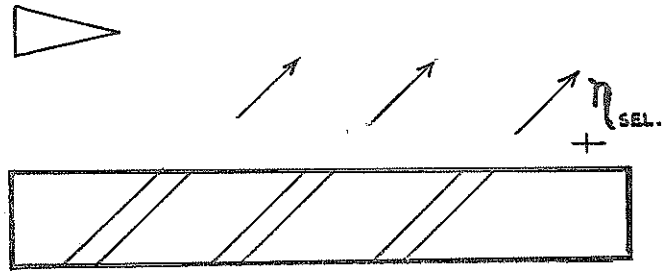

$$\eta_{SEL} = 1. - (1-\eta_1)\cdot(1-\eta_2)\cdot(1-\eta_3)$$

FIG.38

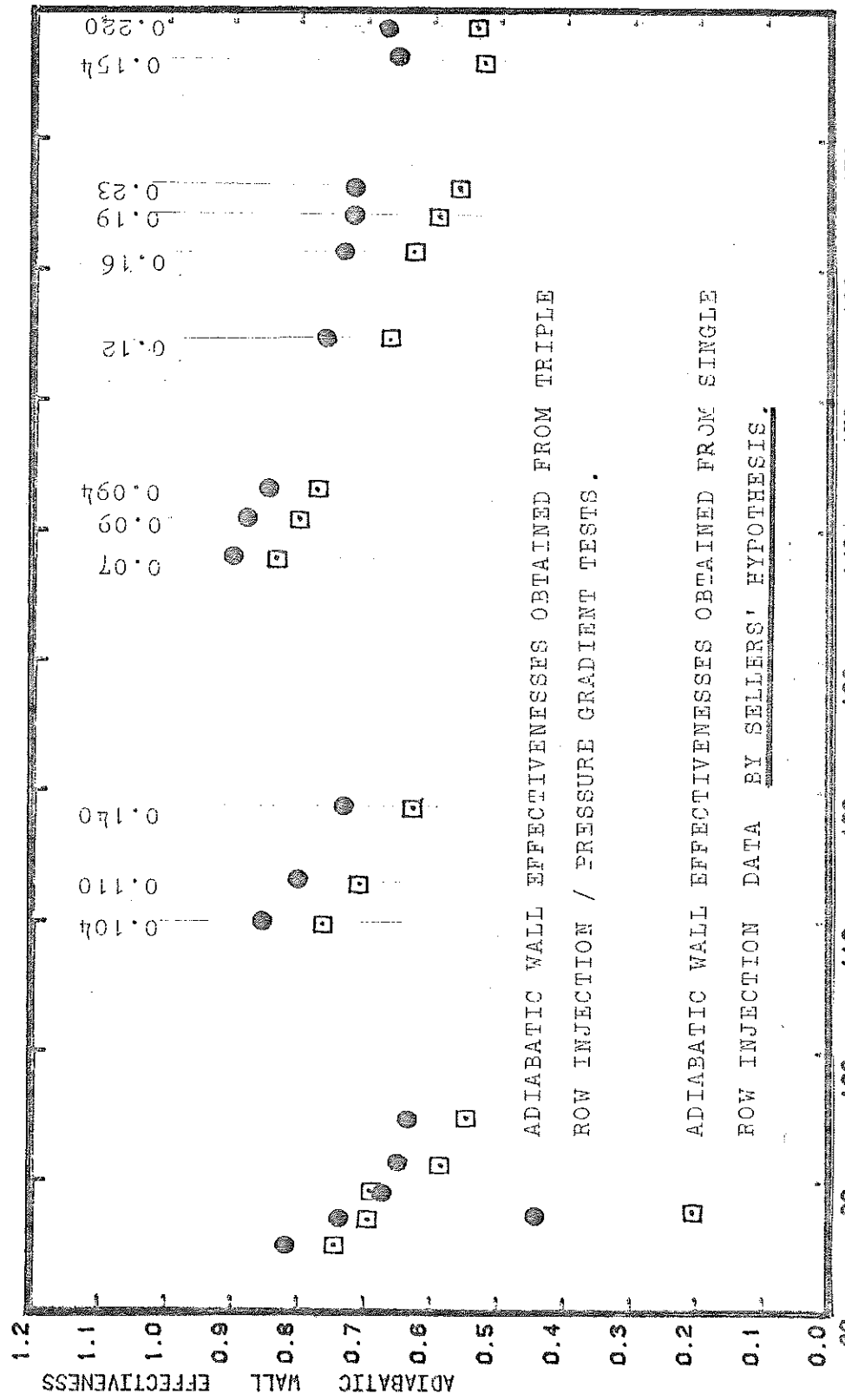

ADIABATIC WALL EFFECTIVENESS DISTRIBUTION OVER THE FLAT PLATE

APPENDIX-I

THERMAL SIMULATION OF ACTUAL GAS TURBINE CONDITIONS

Convection heat transfer coefficient generally depends on a characteristic temperature difference, thermal conductivity, specific heat, density, coordinate, velocity and temperature. This dependency may be written as,

$$Q = f(\Delta T, k, C_p, \rho, x, U, T) \qquad (1)$$

Nusselt number may also be expressed in terms of non-dimensional quantities.

$$Nu = g(Re, Pr, Ma, T/T_s) \qquad (2)$$

T_s is a specified reference temperature.

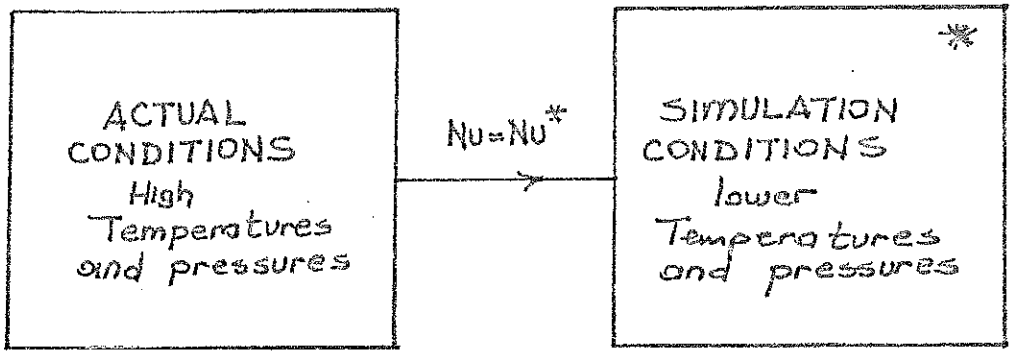

The assumptions made for this problem ;

(7) $Pr = Pr^*$ $\qquad \gamma = \gamma^*$ $\quad (c_p/c_v)$ $\qquad$ (9)

(8) $\dfrac{\mu}{\mu^*} = \dfrac{\sqrt{T}}{\sqrt{T^*}}$ $\qquad R = R^*$ gas constant $\qquad$ (10)

by using the same geometry for both the actual case and the simulation,

$$x = x^* \qquad (11)$$

using eq.(3) and (8)

$$\frac{\rho U . x}{\sqrt{T}} = \frac{\rho^* U^* x^*}{\sqrt{T^*}} \qquad (12)$$

REYNOLDS number simulation

$$\frac{\rho U}{\sqrt{T}} = \frac{\rho^* U^*}{\sqrt{T^*}} \qquad (13)$$

MACH number simulation

$$\frac{U}{\sqrt{T}} = \frac{U^*}{\sqrt{T^*}} \qquad (14)$$

TEMPERATURE RATIO simulation

$$\frac{T}{T_s} = \frac{T^*}{T_s^*} \qquad (15)$$

using equation of state and substituting eq.(10) and (12)

$$P = \rho . R . T \qquad (16)$$

$$P^* = \rho^* R^* T^* \qquad (17)$$

$$\boxed{\frac{P}{P^*} = \frac{T}{T^*} = n} \qquad (18)$$

As an example to this simulation, a total temperature of 1365 °K and a total pressure of 8.75 bar condition were simulated. 'n' was chosen to be 3.5 .Using the analysis given above, simulation conditions were determined.

'n' is a proportionality constant between the actual case and the simulation .

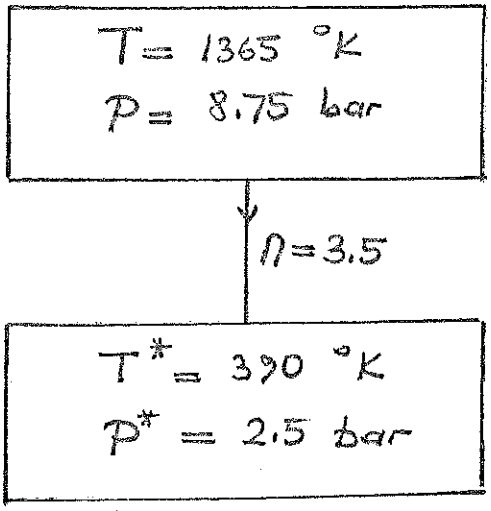

9. PEDERSEN D.R.,ECKERT E.R.G.,GOLDSTEIN R.J. ,'FILM COOLING WITH LARGE DENSITY DIFFERENCES BETWEEN THE MAINSTREAM AND THE SECONDARY FLUID MEASURED BY THE HEAT MASS TRANSFER ANALOGY',ASME Journal of engineering for power,vol:99,November 1977.

10. MUSKA J.F.,FISH R.W.,SUO M.,'THE ADDITIVE NATURE OF FILM COOLING FROM ROWS OF HOLES',ASME Journal of engineering for power,,october 1976 .

11. METZGER D.E.,CARPER H.J.,SWANK L.R.,'HEAT TRANSFER WITH FILM COOLING NEAR NON-TANGENTIAL INJECTION SLOTS',ASME Jornal of engineering for power,1968, pp.157-163 .

12. SCHULTZ D.L.,JONES T.V.,'HEAT TRANSFER MEASUREMENTS IN SHORT DURATION HYPERSONIC FACILITIES', Agardograph no:165 ,February 1973

13. KAYS W.M.,'CONVECTIVE HEAT AND MASS TRANSFER ' McGraw-Hill,Inc. ,1966 .

REFERENCE LIST

1. STRUNCK V., 'EFFECTIVENESS OF FILM COOLING OF SUR_ FACES THROUGH INCLINED HOLES',VKI project report 1979-10,June 1979

2. RICHARDS B.E.,VILLE J.P.,APPELS.C. ,'FILM COOLED SMALL TURBINE BLADE RESEARCH-FILM COOLING EFFEC- TIVENESS AT SIMULATED TURBINE CONDITIONS' ,VKI technical note 120 ,June 1976

3. VILLE J.P.,GODARD M.,RICHARDS B.E.,SIEVERDING C., 'FILM COOLING AND ENDWALL HEAT TRANSFER IN SMALL TURBINE BLADE PASSAGES', VKI Technical Note 126 February 1978 .

4. JABBARI M.V.,GOLDSTEIN R.J.,'ADIABATIC WALL TEMPERA_ TURE AND HEAT TRANSFER DOWNSTREAM OF INJECTION TH_ ROUGH TWO ROWS OF HOLES.' ,ASME Journal of engineering for power,april 1978, vol:100 ,pp:303-307 .

5. AFEJUKU W.O.,HAY.N.,LAMPARD D.,'THE FILM COOLING EFFECTIVENESS OF DOUBLE ROWS OF HOLES',ASME paper 79-GT/Isr-10 .

6. GEORGIOU D.P.,GODARD M.,RICHARDS B.E. ,'EXPERIMENTAL STUDY OF THE ISO-HEAT-TRANSFER LINES ON THE END-WALL OF A TURBINE CASCADE',ASME paper 79-GT-20

7. BLAIR M.F.,'AN EXPERIMENTAL STUDY OF HEAT TRANSFER AND FILM COOLING ON LARGE SCALE TURBINE ENDWALLS', ASME paper 74-GT-33.

8. LANDER R.D.,FISH R.W.,SUO M. ,'EXTERNAL HEAT TRANSFER DISTRIBUTION ON FILM COOLED TURBINE VANES ,Journal of Aircraft,vol:9,no:10,october 1972